NAVAL POSTGRADUATE SCHOOL

MONTEREY, CALIFORNIA

THESIS

INDIUM GALLIUM NITRIDE MULTIJUNCTION SOLAR CELL SIMULATION USING SILVACO ATLAS

by

Baldomero Garcia, Jr.

June 2007

Thesis Advisor: Sherif Michael
Second Reader: Todd Weatherford

Approved for public release; distribution is unlimited

THIS PAGE INTENTIONALLY LEFT BLANK

REPORT DOCUMENTATION PAGE		Form Approved OMB No. 0704-0188

1. AGENCY USE ONLY *(Leave blank)*	2. REPORT DATE June 2007	3. REPORT TYPE AND DATES COVERED Master's Thesis

4. TITLE AND SUBTITLE Indium Gallium Nitride Multijunction Solar Cell Simulation Using Silvaco Atlas	5. FUNDING NUMBERS
6. AUTHOR(S) Baldomero Garcia, Jr.	
7. PERFORMING ORGANIZATION NAME(S) AND ADDRESS(ES) Naval Postgraduate School Monterey, CA 93943-5000	8. PERFORMING ORGANIZATION REPORT NUMBER
9. SPONSORING /MONITORING AGENCY NAME(S) AND ADDRESS(ES) N/A	10. SPONSORING/MONITORING AGENCY REPORT NUMBER

11. SUPPLEMENTARY NOTES The views expressed in this thesis are those of the author and do not reflect the official policy or position of the Department of Defense or the U.S. Government.

12a. DISTRIBUTION / AVAILABILITY STATEMENT Approved for public release; distribution is unlimited	12b. DISTRIBUTION CODE

13. ABSTRACT (maximum 200 words)

This thesis investigates the potential use of wurtzite Indium Gallium Nitride as photovoltaic material. Silvaco Atlas was used to simulate a quad-junction solar cell. Each of the junctions was made up of Indium Gallium Nitride. The band gap of each junction was dependent on the composition percentage of Indium Nitride and Gallium Nitride within Indium Gallium Nitride. The findings of this research show that Indium Gallium Nitride is a promising semiconductor for solar cell use.

14. SUBJECT TERMS Solar cell, photovoltaic device, Indium Gallium Nitride, Silvaco Atlas.	15. NUMBER OF PAGES 113
	16. PRICE CODE

17. SECURITY CLASSIFICATION OF REPORT	18. SECURITY CLASSIFICATION OF THIS PAGE	19. SECURITY CLASSIFICATION OF ABSTRACT	20. LIMITATION OF ABSTRACT
Unclassified	Unclassified	Unclassified	UL

NSN 7540-01-280-5500 Standard Form 298 (Rev. 2-89)
Prescribed by ANSI Std. 239-18

THIS PAGE INTENTIONALLY LEFT BLANK

Approved for public release; distribution is unlimited

INDIUM GALLIUM NITRIDE MULTIJUNCTION SOLAR CELL SIMULATION USING SILVACO ATLAS

Baldomero Garcia, Jr.
Lieutenant Commander, United States Navy
B.S., U.S. Naval Academy, 1995

Submitted in partial fulfillment of the
requirements for the degree of

MASTER OF SCIENCE IN ELECTRICAL ENGINEERING

from the

NAVAL POSTGRADUATE SCHOOL
June 2007

Author: Baldomero Garcia, Jr.

Approved by: Sherif Michael
Thesis Advisor

Todd Weatherford
Second Reader

Jeffrey B. Knorr
Chairman, Department of Electrical and
Computer Engineering

THIS PAGE INTENTIONALLY LEFT BLANK

ABSTRACT

This thesis investigates the potential use of wurtzite Indium Gallium Nitride as photovoltaic material. Silvaco Atlas was used to simulate a quad-junction solar cell. Each of the junctions was made up of Indium Gallium Nitride. The band gap of each junction was dependent on the composition percentage of Indium Nitride and Gallium Nitride within Indium Gallium Nitride. The findings of this research show that Indium Gallium Nitride is a promising semiconductor for solar cell use.

THIS PAGE INTENTIONALLY LEFT BLANK

TABLE OF CONTENTS

LIST OF FIGURES

LIST OF TABLES

THIS PAGE INTENTIONALLY LEFT BLANK

ACKNOWLEDGMENTS

First, I would like to thank Professor Sherif Michael for his help and guidance during the research process. His insight was invaluable when faced with difficult problems.

Second, I would like to thank Professor Todd Weatherford for clarifying issues regarding the use of Silvaco Atlas. He was also critical in finding points of contact at Lawrence Berkeley Laboratory.

Third, I would like to thank Dr. Wladek Walukiewicz from the Material Sciences Division at Lawrence Berkeley National Laboratory. He and his team are the world-wide leaders in Indium Gallium Nitride material science research. Their research was my inspiration to start this research project.

Fourth, I would like to thank Dr. Petra Specht from Lawrence Berkeley National Laboratory. She provided key data used in this research.

And last, but not least, I would like to thank my wife, Nozomi and our children, Oscar and Yuuki, for their patience and support during my time at the Naval Postgraduate School.

THIS PAGE INTENTIONALLY LEFT BLANK

EXECUTIVE SUMMARY

One of the primary goals of solar cell design is to improve efficiency. Indium Gallium Nitride is a material that has undergone extensive research since 2002 as a potential photovoltaic material. By varying the composition of Indium Nitride and Gallium Nitride within Indium Gallium Nitride, the band gap of this semiconductor material can be changed. The band gap range of Indium Gallium Nitride matches closely the visible solar spectrum frequencies. Hence, a high-efficiency solar cell can be potentially developed by having several Indium Gallium Nitride junctions.

The use of Silvaco Atlas as a simulation tool can aid in identifying whether Indium Gallium Nitride can be used for photovoltaics. Previous research at the Naval Postgraduate School has demonstrated the viability of Silvaco Atlas as a solar cell modeling mechanism.

Finding high-efficiency solar cell models is of great interest in space applications. By increasing the efficiency of photovoltaics, the number of solar panels is decreased. Therefore, the overall weight that needs to be launched into space is reduced. A cost-reduction can be achieved over the life of the space power system.

Research at Lawrence Berkeley National Laboratory (LBNL) has been ongoing since 2002 in trying to develop high-efficiency solar cells. One of the materials LBNL has been investigating is Indium Gallium Nitride. In addition to the band gap range, Indium Gallium Nitride also has other characteristics that are beneficial for space applications.

The radiation level that Indium Gallium Nitride is able to withstand is approximately two orders of magnitude greater than current multijunction solar cell materials. Therefore, it is of great interest to continue to research Indium Gallium Nitride and its possibilities as photovoltaic material.

The goal of this research was to investigate the efficiency of Indium Gallium Nitride solar cells using the Silvaco Atlas TCAD simulation software. No other TCAD simulations have been performed on InGaN solar cells. The methodology of this research progressed from single to multi-junction cells. The simulation results predicted efficiencies as high as 41% for a four-junction solar cell. Further refinements of the simulation model are still possible. Actual production of a single-junction solar cell is the next step required to eventually manufacture high-efficiency, multi-junction InGaN solar cells.

I. INTRODUCTION

A. BACKGROUND

One of the most important problems to solve in space solar cell design is efficiency. As efficiency increases, the required number of cells decreases to fulfill electrical power requirements.

Solar cell efficiencies have improved over time by increasing the number of junctions. Each junction is capable of extracting energy from a portion of the solar spectrum.

A new path to improving efficiency is to use new photovoltaic materials such as wurtzite Indium Gallium Nitride. Indium Gallium Nitride possesses a band gap range that can extract energy from a large portion of the visible solar spectrum.

B. OBJECTIVE

The objective of this thesis is to simulate Indium Gallium Nitride solar cells to predict their efficiencies. After obtaining the efficiencies, a comparison is made with current solar cell efficiencies. Silvaco Atlas TCAD simulation software is used to investigate these efficiencies.

C. RELATED WORK

Previous Silvaco Atlas solar cell simulations have been performed by Naval Postgraduate School researchers. Michalopoulos [1] investigated the feasibility of designing solar cells using Silvaco Atlas. To demonstrate the use of

Silvaco Atlas, Michalopoulos simulated single-junction solar cells with Gallium Arsenide, dual-junction solar cells with Indium Gallium Phosphide and Gallium Arsenide, and triple-junction cells with Indium Gallium Phosphide, Gallium Arsenide, and Germanium. The highest efficiency obtained with the triple-junction was 29.5%. This result matched the 29.3% efficiency obtained with actual triple-junction solar cells in production. Bates [2] provided excellent background on the use of Silvaco Atlas. Green [3] and Canfield [4] continued to work on Silvaco Atlas solar cell design. Matlab functions and Silvaco Atlas code were modified from [1]-[4] to perform simulations in this research.

A previous Indium Gallium Nitride simulation has been performed [5] using fundamental semiconductor physics formulas. The results of this research are compared with those of [5].

D. ORGANIZATION

1. Purpose of Solar Cells

The purpose of solar cells is to convert light energy into electrical energy. Light is made up of photons. Photons carry energy that is dependent on the color, or wavelength of light. Electrical energy is generated when photons excite electrons from the valence band into the conduction band in semiconductor materials. Chapter II covers fundamental concepts of solar cells and semiconductor materials.

2. Simulation Software

Silvaco Atlas was used as the simulation software in this thesis. Silvaco offers a suite of software programs

that can act as a Virtual Wafer Fabrication (VWF) tool. The Naval Postgraduate School has had multiple researchers publish theses on the use of Silvaco Atlas for the purpose of solar cell modeling. Chapter III covers the basics of Silvaco Atlas.

3. Indium Gallium Nitride

Wurtzite Indium Gallium Nitride (InGaN) is a semiconductor that has the potential to produce high-efficiency solar cells. Dr. Wladek Walukiewicz, of Lawrence Berkeley National Laboratory (Solar Energy Materials Research Group), has been conducting extensive InGaN research for the purposes of producing photovoltaic material. Chapter IV covers the characteristics of InGaN, its potential, its material science research status, and its current limitations.

4. Simulation

Based on the optical characteristics of InGaN, simulations were performed using Silvaco Atlas. Chapter V covers the findings of the simulations. Chapter VI covers the conclusions and recommendations. Finally, the appendices include the code used in Silvaco Atlas as well as Matlab.

THIS PAGE LEFT INTENTIONALLY BLANK

II. SOLAR CELL AND SEMICONDUCTOR BASICS

This thesis examines a novel process to simulate Indium Gallium Nitride solar cells. Before delving into the simulation, this chapter covers the fundamental principles of solar cells and semiconductors. The properties of the semiconductor material determine the characteristics of the photovoltaic device.

A. SEMICONDUCTOR FUNDAMENTALS

1. Classification of Materials

Materials can be categorized according to their electrical properties as conductors, insulators or semiconductors. The conductivity σ is a key parameter in identifying the type of material.

Figure 1 presents a sample of materials based on conductivity. The semiconductors fall between the insulators and the conductors.

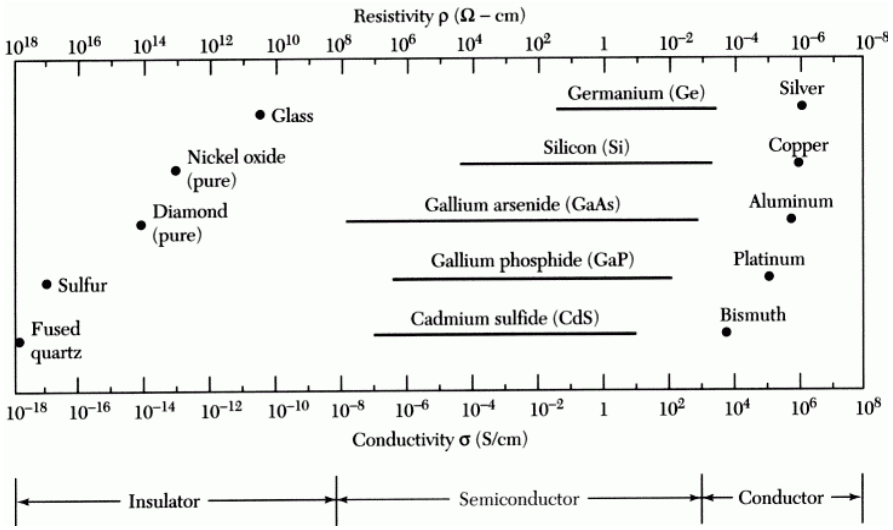

Figure 1. Materials classified by conductivity (From [6]).

Semiconductors can be found in elemental or compound form. Silicon (Si) and Germanium (Ge) are examples of elemental semiconductors. Both of these semiconductors belong to group IV of the periodic table.

Figure 2 shows an abbreviated periodic table. In addition to the group IV semiconductors, compounds can be made with elements from groups III and V, respectively. Examples of III-V semiconductors include Aluminum Phosphide (AlP), Gallium Nitride (GaN), Indium Phosphide (InP), Gallium Arsenide (GaAs), among others. It is also possible to make semiconductor compounds from groups II-VI, such as Zinc Oxide (ZnO), Cadmium Telluride (CdTe), Mercury Sulfide (HgS), among others. The subject of this thesis is the ternary alloy wurtzite Indium Gallium Nitride (InGaN). Indium and Gallium are group III elements, while Nitrogen is a group V element.

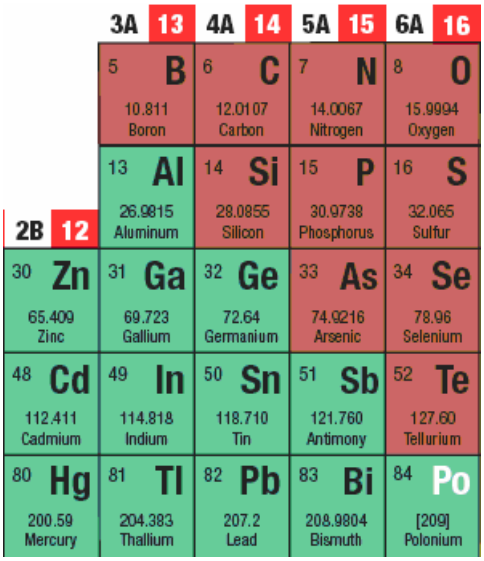

Figure 2. Partial periodic table (After [7]).

2. Atomic Structure

Since Silicon is the most commonly used semiconductor in solar cells today, a brief analysis of this element is presented.

Silicon has 14 protons and 14 neutrons in its nucleus. The 14 electrons are distributed in three shells.

Figure 3 shows the arrangement of electrons in a Silicon atom. There are two electrons in the first shell, eight electrons in the second shell and four electrons in the outer shell. When Silicon atoms are together, the atoms from the outer shells form covalent bonds. Hence, a Silicon atom forms bonds with four other Silicon atoms.

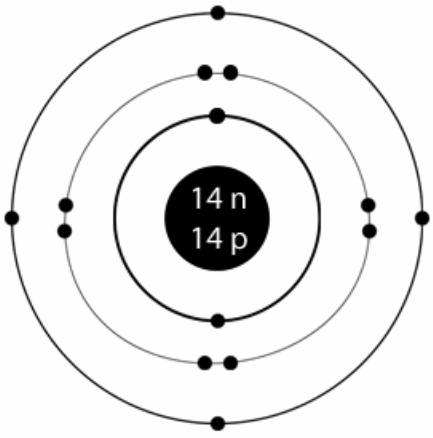

Figure 3. Silicon atomic structure (From [8]).

As shown in Figure 4, the covalent bonds formed by the silicon atoms are represented by the elliptical dotted lines. In the absence of an electron, the covalent bond ceases to exist. A hole takes the place of the electron.

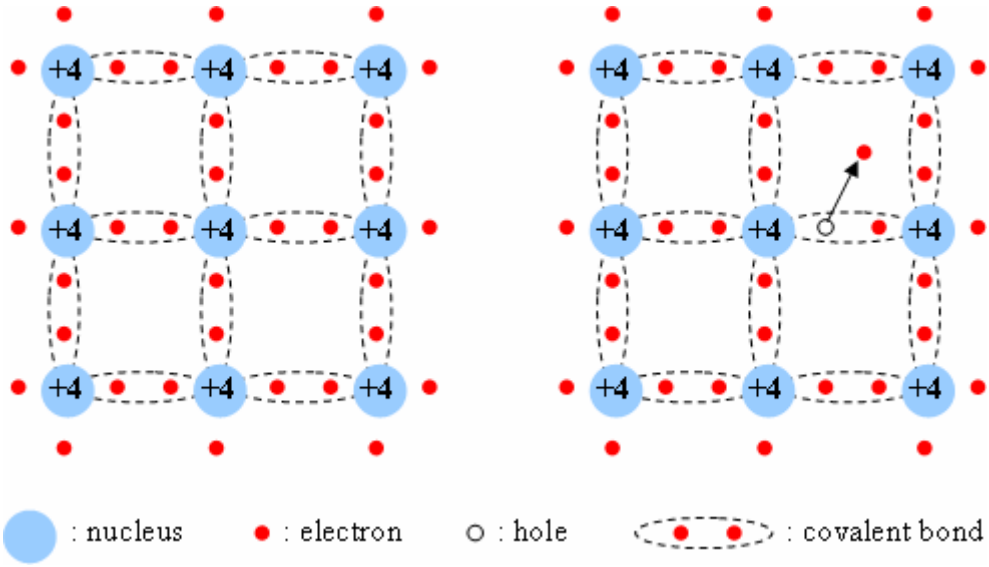

Figure 4. Silicon atom covalent bonds (From [1, p. 11]).

Energy bands are a fundamental concept of semiconductor physics. These energy bands are the valence band, the conduction band, and the forbidden gap or band gap [9, p. 27]. When an electron is in the valence band, the covalent bond exists. In order for the electron to move from the valence band into the conduction band, energy is required to excite the electron. The band gap energy is the minimum energy required for the electron to make the move from the valence band into the conduction band.

Figure 5 shows the band gap diagrams for conductors, insulators, and semiconductors. This figure also reinforces the differences among the three types of materials according to their electric properties. In the case of conductors, the band gap is small or non-existent. By contrast, insulators have wide band gaps. Therefore, it takes much more energy for the insulator to have electrons in the conduction band.

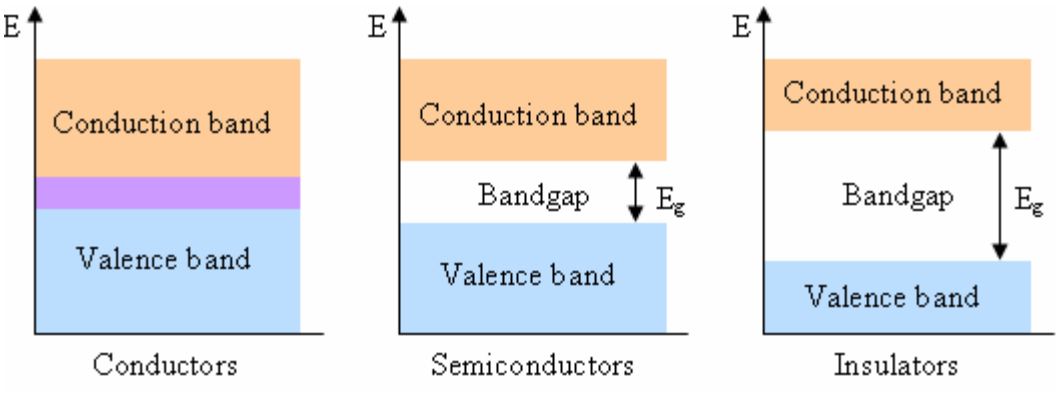

Figure 5. Band gap diagrams (From [1, p. 8]).

Semiconductors have band gaps that are dependent on the material. Because band gap is also dependent on temperature, it should be noted that all quoted band gaps in this thesis are at room temperature (300 K.)

3. Electrons and Holes

A semiconductor at absolute zero temperature is unable to conduct heat or electricity [10, p. 44]. All of the semiconductor's electrons are bonded. The electrons acquire kinetic energy as the temperature is increased. Some of the electrons are freed and move into the conduction band. These electrons are able to conduct charge or energy. The areas left by these electrons in the valence band are called holes. As the temperature of the semiconductor increases, the number of free electrons and holes increases as well. Therefore, the conductivity of the semiconductor is directly proportional to temperature increases.

The conductivity of the semiconductor can be altered by exposing it to light or by doping it. Photoconductivity consists of exposing the semiconductor with photon energy

larger than the semiconductor's band gap. Doping consists of adding impurities to the semiconductor material.

Figure 6 shows n-type and p-type doping. The atom of the semiconductor is represented by the blue circle and a +4. For example, a silicon atom has four electrons in its outer shell. When silicon atoms are n-doped, atoms from group V of the periodic table are added. Each added group V atom provides an extra electron to donate. When silicon atoms are p-doped, the atoms from group III of the periodic table are added. Each group III atom has one less electron than silicon. Therefore, a hole is added. Doping increases the number of carriers in the semiconductor material.

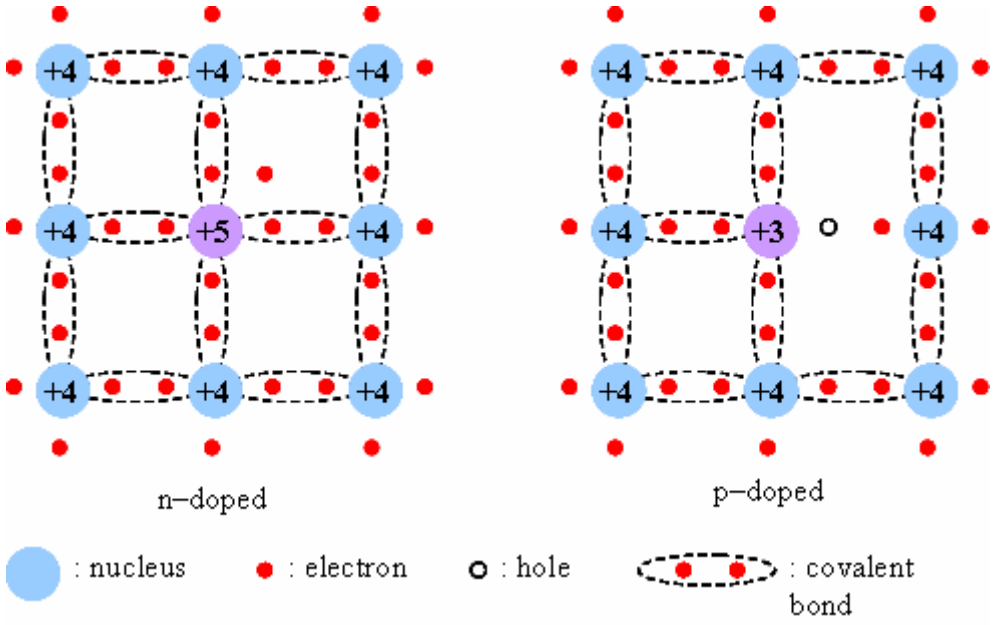

Figure 6. Doping: n-type and p-type (From [1, p. 13]).

An intrinsic semiconductor is a pure semiconductor with a negligible amount of impurity atoms [9, p.34]. By definition, the number of electrons and holes in a semiconductor are represented by n and p. See Table 1.

$$n = \frac{\text{number of electrons}}{\text{cm}^3}$$
$$p = \frac{\text{number of holes}}{\text{cm}^3}$$

Table 1. Definitions of n and p.

In the case of an intrinsic semiconductor, the following case occurs:

$$n = p = n_i$$

For example purposes, n_i is given for GaAs, Si and Ge and room temperature [9, p.34]. Data for InN and GaN are from [11]. See Table 2.

$$n_i^{GaAs} = \frac{2\times10^6}{cm^3}$$
$$n_i^{Si} = \frac{1\times10^{10}}{cm^3}$$
$$n_i^{Ge} = \frac{2\times10^{13}}{cm^3}$$
$$n_i^{InN} = \frac{6.2\times10^{22}}{cm^3}$$
$$n_i^{GaN} = \frac{8.9\times10^{22}}{cm^3}$$

Table 2. n_i for five semiconductors.

When solar cells utilize semiconductor materials from Table 2, the current level is highest for Ge and lowest for GaAs. The current levels correspond in rank to the n_i levels provided in Table 2. No data exists for InN or GaN current levels as photovoltaic materials.

4. Direct and Indirect Band Gaps

Since the band gap is the minimum energy required to move an electron from the valence band into the conduction band, it is necessary to distinguish between direct and indirect band gaps.

Figure 7 shows the concept of direct and indirect band gaps. The blue portion represents the valence band. The tan portion represents the conduction band.

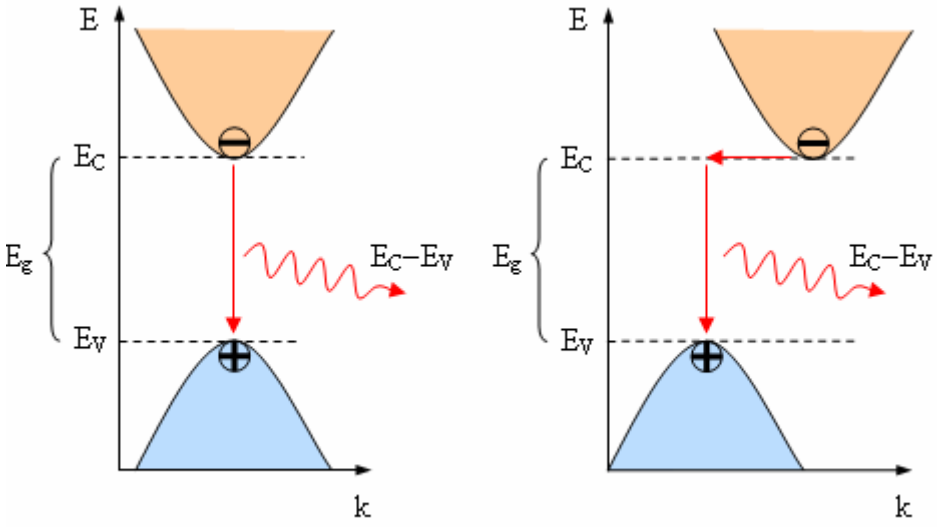

Figure 7. Direct and indirect band gaps (After [1, p. 24]).

When the valence band and the conduction band coincide in wave vector k, the semiconductor has a direct band gap. When the valence band and the conduction band have different wave vector k, the semiconductor has an indirect band gap. The k vector represents a difference in momentum. Photons have negligible momentum. In order to excite an electron from the valence band to the conduction band in an indirect band gap semiconductor, in addition to a photon, a phonon is required. The phonon is a lattice vibration. The phonon

transfers its momentum to the electron at the time the photon is absorbed. Therefore, a direct band gap semiconductor is generally better for optoelectronics. Silicon is an example of an indirect band gap semiconductor. Gallium Arsenide and wurtzite Indium Gallium Nitride are examples of direct band gap semiconductors.

5. Fermi Level

The Fermi function f(E) specifies how many of the existing states at energy E are filled with an electron [9, p.42]. The Fermi function is a probability distribution function defined as follows:

$$f(E)=\frac{1}{1+e^{\frac{(E-E_F)}{kT}}}$$

Where E_F is the Fermi level, k is Boltzmann's constant, and T is the temperature in Kelvin.

From the Fermi function, it can be determined that when $E=E_F$, then $f(E)=f(E_F)=0.5$.

Figure 8 shows the Fermi level for an intrinsic semiconductor. Figure 9 shows the Fermi level for n-type semiconductor. Figure 10 shows the Fermi level for p-type semiconductor. From these Figures, it can be deduced that the n-type material has a larger electron carrier distribution and the p-type material has a larger hole carrier distribution.

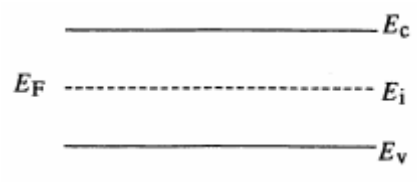

Figure 8. Fermi level: intrinsic case (After [9, p. 42]).

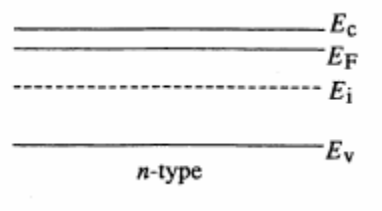

Figure 9. Fermi level: n-type case (After [9, p. 42]).

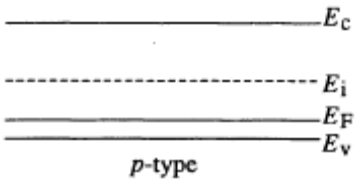

Figure 10. Fermi level: p-type case (After [9, p. 42]).

B. SOLAR CELL FUNDAMENTALS

After covering the basics of semiconductors, the logical step is to continue with solar cell fundamentals.

1. History of Solar Cells

Solar cell research started when Edmund Bequerel discovered the photovoltaic effect in 1839. He recorded that an electric current was produced when light was applied to a silver coated platinum electrode immersed in electrolyte. The next significant step was performed by William Adams and Richard Day in 1876. They discovered that a photocurrent appeared when selenium was contacted by two heated platinum contacts. However, current was produced spontaneously by the action of light. Continuing to build on these efforts, Charles Fritts developed the first large area solar cell in 1894. He pressed a layer of selenium between gold and another metal. Progress continued as the theory of metal-

semiconductor barrier layers was established by Walter Schottky and other. In the 1950s, silicon was used for solid state electronics. Silicon p-n junctions were used to improve on the performance of the Schottky barrier. These silicon junctions had better rectifying action and photovoltaic behavior. In 1954, Chapin, Fuller and Pearson developed the first silicon solar cell, with a reported efficiency of 6%. However, the cost per Watt associated with these solar cells made them prohibitively expensive for terrestrial use. However, locations where power generation was not feasible (i.e., space) were suitable for solar cells. Satellites were the first clear application for silicon solar cells. Since that time, solar cells have progressed steadily both in terms of efficiency as well as materials used their production [10, p. 2].

Table 3 shows a brief list of events in the history of photovoltaics from 1939 until 2002.

2. The Photovoltaic Effect

The photovoltaic effect is the process by which a solar cell converts the energy from light into electrical energy. Light is made up of photons. The energy of these photons depends on the color (wavelength) of light. The material that makes up the solar cell determines the photovoltaic properties when light is applied [10, p. 1].

When light is absorbed by matter, such as metal, photons provide the energy for electrons to move to higher energy states within the material. However, the excited electrons return to their original energy state. In semiconductor materials, there is a built-in asymmetry (band

gap). This allows the electrons to be transferred to an external circuit before they can return to their original energy state. The energy of the excited electrons creates a potential difference. This electromotive force directs the electrons through a load in the external circuit to perform electrical work.

- 1839 Becquerel (FR) discovered photogalvanic effect in liquid electrolytes
- 1873 Smith (UK) discovered photoconductivity of solid Se
- 1877 Adams and Day (UK) discover photogeneration of current in Se tubes; the first observation of PV effect in solids
- 1883 Fritts (US) makes first large area solar cell using Se film
- 1954 First 6% efficient solar cells reported: Si (Bell Lab, USA) and Cu_2S/CdS (Air Force, USA)
- 1955 Hoffman Electronics (USA) offers 2% efficient Si PV cells at $1500/W
- 1958 NASA Vanguard satellite with Si backup solar array
- 1959 Hoffman Electronics (USA) offers 10% efficient Si PV cells
- 1963 Sharp Corp (JP) produces first commercial Si modules
- 1966 NASA Orbiting Astronomical Observatory launched with 1 kW array
- 1970 First GaAs heterostructure solar cells by Alferov, Andreev *et al.* in the USSR
- 1972 First PV conference to include a session on terrestrial applications (IEEE)
- 1973 A big year in photovoltaics: Worldwide oil crisis spurs many nations to consider renewable energy including photovoltaics; Cherry Hill Conference in USA (established photovoltaics' potential and legitimacy for government research funding); World's first solar powered residence (University of Delaware, USA) built with Cu_2S (not c-Si!) solar modules
- 1974 Project Sunshine initiated in Japan to foster growth of PV industry and applications; Tyco (USA) grows 2.5 cm wide Si ribbon for photovoltaics, first alternative to Si wafers
- 1975 First book dedicated to PV science and technology by Hovel (USA)
- 1980 First thin-film solar cell >10% using Cu_2S/CdS (USA)
- 1981 350 kW Concentrator array installed in Saudi Arabia
- 1982 First 1 MW utility scale PV power plant (CA, USA) with Arco Si modules on 2-axis trackers
- 1984 6 MW array installed in Carrisa Plains CA, USA [35]
- 1985 A big year for high-efficiency Si solar cells: Si solar cell >20% under standard sunlight (UNSW, Australia) [36] and >25% under 200X concentration (Stanford Univ. USA) [37]
- 1986 First commercial thin-film power module, the a-Si G4000 from Arco Solar (USA)
- 1987 Fourteen solar powered cars complete the 3200 km World Solar Challenge race (Australia) with the winner averaging 70 kph
- 1994 GaInP/GaAs 2-terminal concentrator multijunction >30% (NREL, USA) [38]
- 1995 "1000 roofs" German demonstration project to install photovoltaics on houses, which triggered the present favorable PV legislation in Germany, Japan and other countries
- 1996 Photoelectrochemical "dye-sensitized" solid/liquid cell achieves 11% (EPFL, Switzerland) [39]
- 1997 Worldwide PV production reaches 100 MW per year
- 1998 Cu(InGa)Se_2 thin-film solar cell reaches 19% efficiency (NREL, US) [40] comparable with multicrystalline Si. First concentrating array for space launched on Deep Space 1 by US (5 kW using high efficiency GaInP/GaAs/Ge triple junction cells)
- 1999 Cumulative worldwide installed photovoltaics reaches 1000 MW
- 2000 Olympics in Australia highlight wide range of PV applications, and the awarding of the first Bachelor of Engineering degrees in Photovoltaics and Solar Engineering (UNSW, Australia)
- 2002 Cumulative worldwide installed photovoltaics reaches 2000 MW. It took 25 years to reach the first 1000 MW and only 3 years to double it; production of crystalline Si cells exceeds 100 MW per year at Sharp Corp. (Japan). BP Solar ceases R&D and production of a-Si and CdTe thin-film modules in USA ending >20 years of effort

Table 3. Notable events in the history of photovoltaics (From [12]).

a. The Electromagnetic Spectrum

Light is electromagnetic radiation. The frequency of light determines its color. Figure 11 shows the visible part of the electromagnetic spectrum. Visible wavelengths range from 390 nm (violet) to 780 nm (red).

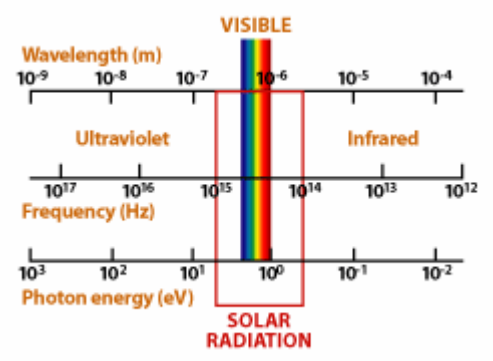

Figure 11. The electromagnetic spectrum (From [13]).

Table 4 shows the approximate wavelength range of visible colors.

Color	Wavelength (nm)
Red	780-622
Orange	622-597
Yellow	597-577
Green	577-492
Blue	492-455
Violet	455-390

Table 4. Approximate wavelength of various colors in vacuum (After [14]).

The sun emits light from ultraviolet, visible, and infrared wavelengths in the electromagnetic spectrum. Solar irradiance has the largest magnitude at visible wavelengths, peaking in the blue-green [10, p. 17].

b. Band Gap

The band gap of the semiconductor material determines how the solar cell reacts to light. Table 5 shows a small sample of semiconductor band gaps. Chapter IV covers the band gaps of Indium Nitride, Gallium Nitride, and Indium Gallium Nitride.

Material	**Band gap (eV) at 300 K**
Si	1.12
Ge	0.66
GaAs	1.42
InP	1.34

Table 5. Common semiconductor band gaps (After [9, p. 31]).

The band gap of the semiconductor material determines the wavelength of light that meet the requirements to generate electrical energy. The conversion formula between band gap and wavelength is:

$$\lambda(\mu m) = \frac{hc}{Eg(eV)}$$

$$\lambda(\mu m) = \frac{1.24}{Eg(eV)}$$

Where λ is the wavelength in micrometers, h is Planck's constant, c is the speed of light in vacuum, and Eg

is the band gap in eV. One eV is approximately equal to $1.6x10^{-19}$ J of energy. In the case of Gallium Arsenide, the wavelength that corresponds to 1.42 eV is 0.873 μm.

Figure 12 helps visualize the concept of light absorption. When light has energy greater than 1.1 eV, the silicon solar cell generates electricity. Light with less than 1.1 eV of energy is unused. Similarly, light with energy greater than 1.43 eV excites the outer shell electrons of the gallium arsenide solar cell. And finally, light with energy greater than 1.7 eV is useful for aluminum gallium arsenide photovoltaic material.

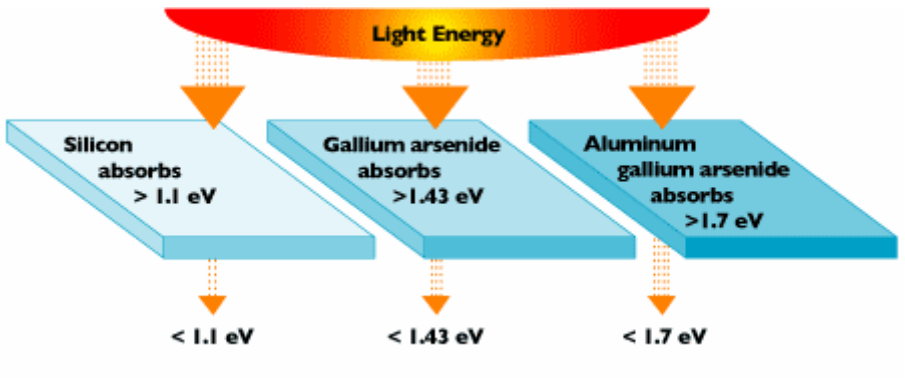

Figure 12. Effect of light energy on different band gaps (From [15]).

c. Solar Cell Junctions

The discussion in the previous section discussed the effect of light energy on different band gaps. Treated individually, each of the photovoltaic materials from Figure 12 would act as a single junction solar cell.

However, to increase the efficiency of the solar cell, multiple junctions can be created. For example, in

Figure 12, the top junction would be made up of Aluminum Gallium Arsenide. This junction would absorb light energy greater than 1.7 eV. Any unused photons would be filtered through to the next junction. The gallium arsenide junction would then absorb the photons with energy greater than 1.4 eV. The remaining photons would be absorbed by the silicon junction.

Although the above paragraph described the basics of a multijunction solar cell, such device may not produce the desired results due to lattice mismatch. The next section covers the basics of lattice matching.

d. Lattice Matching

Semiconductors are three-dimensional in their cell structure. The simple cubic structure serves to illustrate the concept of lattice and is presented in Figure 13.

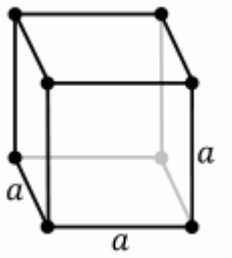

Figure 13. Simple cubic lattice structure (From [16]).

Figure 13 shows that each side of the cube is represented by the letter “a”. The separation “a” is called the lattice constant. Each semiconductor material has a lattice constant. Therefore, when creating multijunction solar cells, the lattices must be matched.

Figure 14 shows the lattice constants for several semiconductors. An example given by P. Michalopoulos [1, p. 87] shows how to lattice match Indium Gallium Phosphide to Gallium Arsenide.

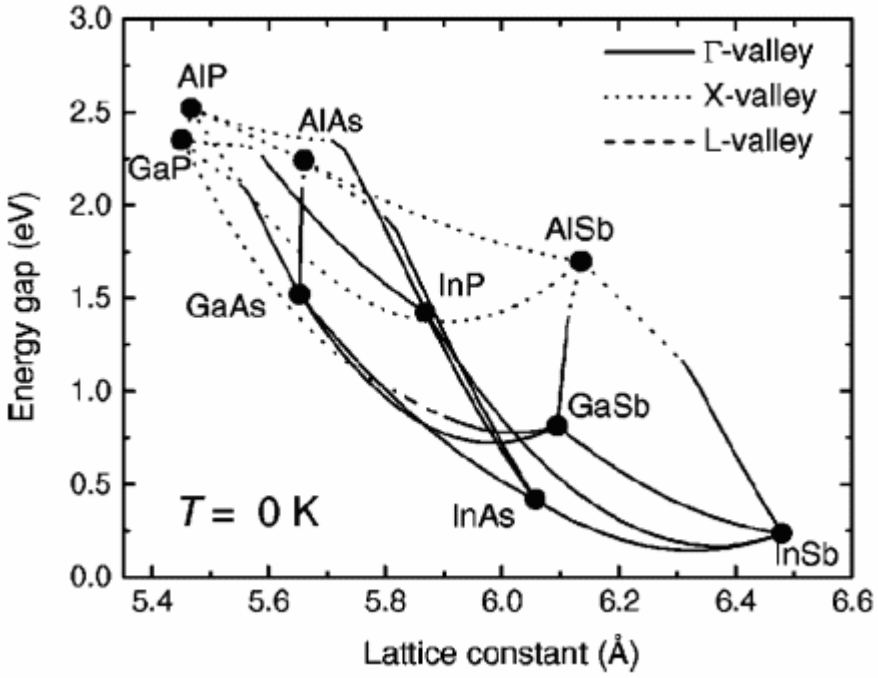

Figure 14. Lattice constants (From [17]).

The alloy Indium Gallium Phosphide is composed of x parts of Gallium phosphide and 1-x parts of Indium Phosphide. Therefore, Indium Gallium Phosphide is represented as $In_{1-x}Ga_xP$.

GaAs has a lattice constant α=5.65Å, GaP has α=5.45Å and InP has α=5.87Å. The goal is to create InGaP with a lattice constant that matches that of GaAs. The formula to find x is given as:

$$\alpha_{GaAs} = \alpha_{GaP} \cdot x + \alpha_{InP} \cdot (1-x) \Leftrightarrow x = \frac{\alpha_{GaAs} - \alpha_{InP}}{\alpha_{GaP} - \alpha_{InP}}$$

With x=0.52, $In_{0.48}Ga_{0.52}P$ has α=5.65Å. A rough approximation of the resulting band gap of $In_{0.48}Ga_{0.52}P$ is given as follows:

$$E_G^{InGaP} = xE_G^{GaP} + (1-x)E_G^{InP}$$

The equation yields a band gap of 1.9 eV for $In_{0.48}Ga_{0.52}P$. Therefore, a dual-junction solar cell of InGaP at 1.9 eV and GaAs at 1.4 eV can be built.

Figure 15 shows the lattice constant for Indium Nitride and Gallium Nitride.

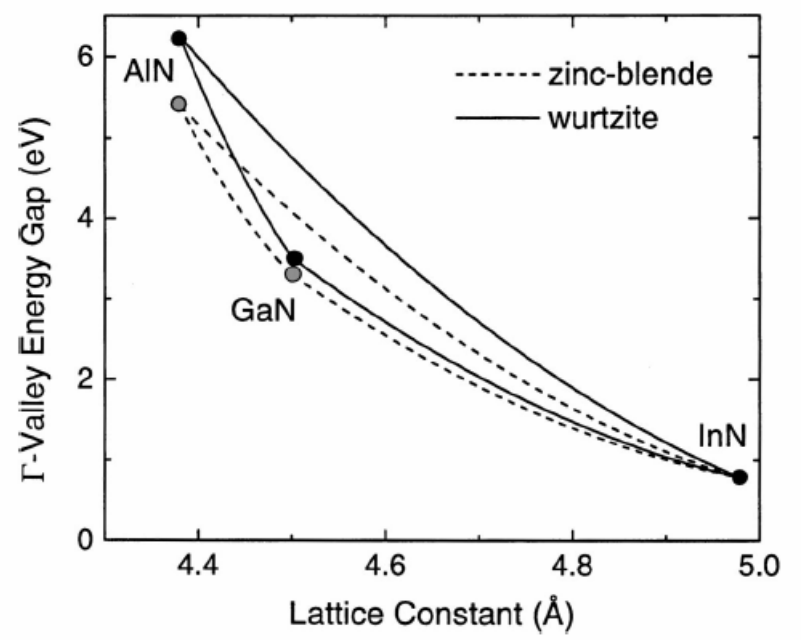

Figure 15. Lattice constant for InN and GaN (From [18]).

e. AM0 Spectrum

The location of the solar cell affects the input solar radiation spectrum. A solar cell on Mars receives a

different (smaller) spectrum than a solar cell on a satellite that orbits Earth. The energy received outside Earth's atmosphere is approximately 1365 W/m^2. This spectrum is called Air Mass Zero or AM0. Terrestrial solar cells have to deal with the attenuation of the solar spectrum due to Earth's atmosphere. This solar spectrum is called AM1.5. For the purposes of this thesis, AM0 is used during simulations. From data obtained from the National Renewable Energy Laboratory (NREL) [19], the AM0 spectrum was plotted using a Matlab script.

Figures 16 and 17 show the AM0 spectrum with respect to wavelength and energy, respectively. From Figure 17, it can be seen that semiconductor materials with band gaps of less than 4 eV are able to extract most of the solar spectrum.

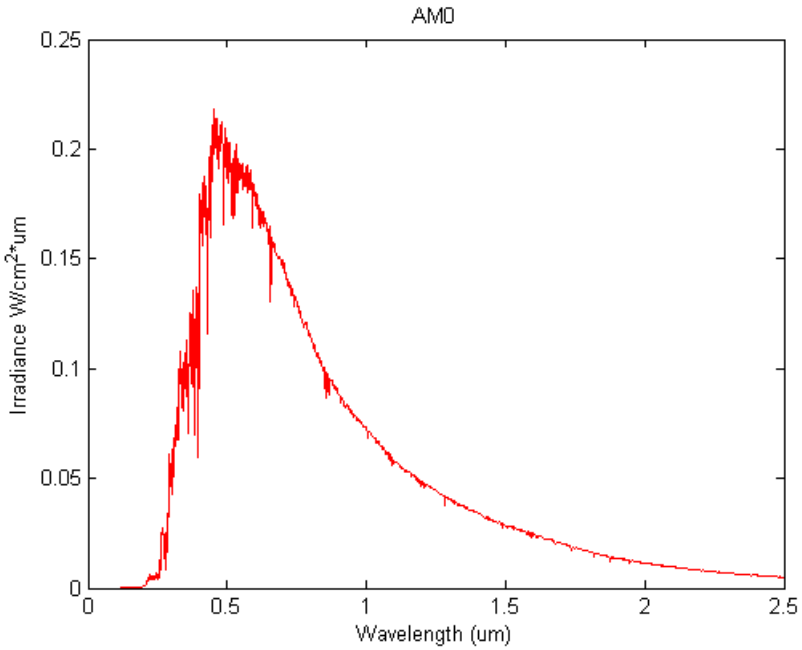

Figure 16. AM0 spectrum (Wavelength vs Irradiance) (After [19]).

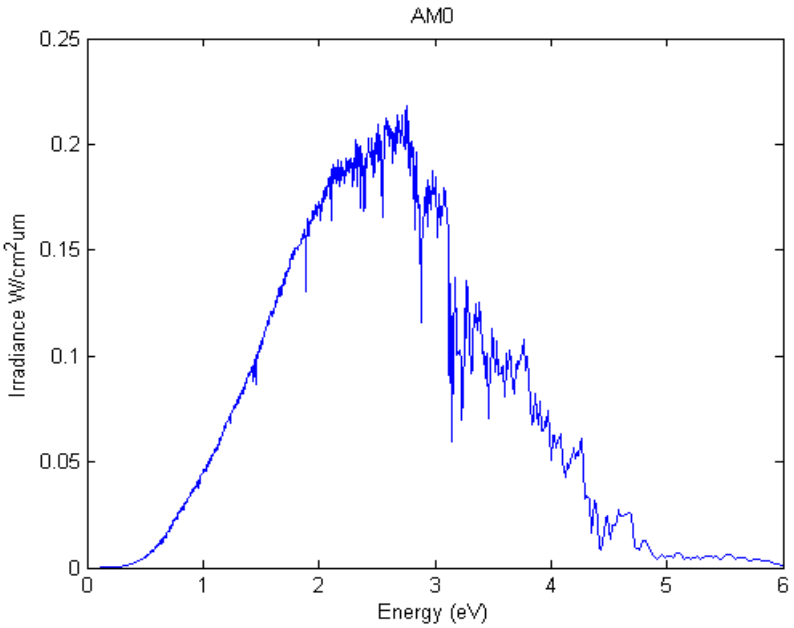

Figure 17. AM0 spectrum (Energy vs Irradiance) (After [19]).

f. Current-Voltage Curves

A typical solar cell current-voltage (IV) curve is presented in Figure 18.

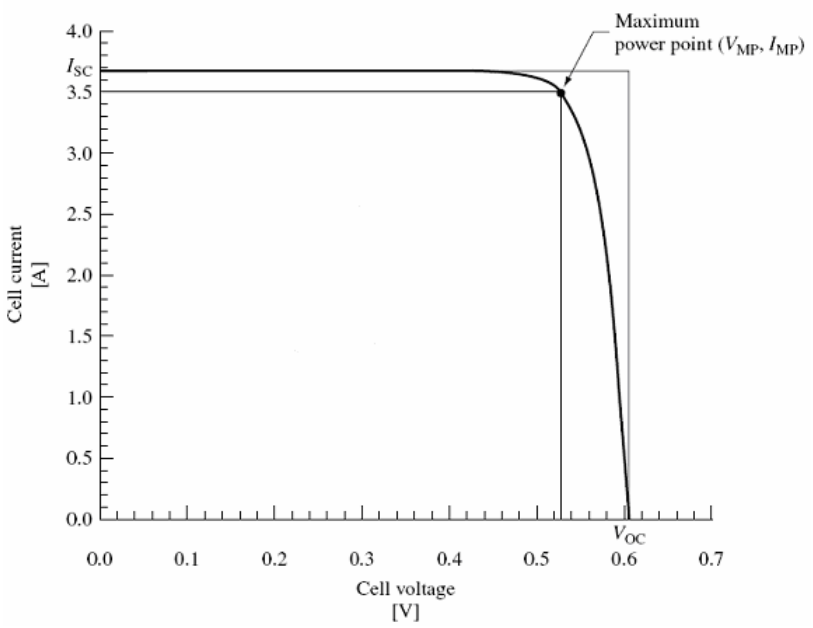

Figure 18. Sample IV curve used in efficiency calculations (After [20]).

From Figure 18, there are several points of interest. The short circuit current (I_{SC}) occurs when the voltage is zero. This is the highest absolute value current. The open circuit voltage (V_{OC}) occurs when the current is zero. This is the highest voltage. The dimensions of the larger rectangle in Figure 18 are determined by V_{OC} and I_{SC}. Since power (P) is determined by the product of current times voltage, the maximum power point occurs at (V_{MP},I_{MP}).

The calculations for solar cell efficiency are as follows:

$$P_{max}=I_{mp}V_{mp}$$

$$FF=\frac{P_{max}}{I_{sc}V_{oc}}=\frac{I_{mp}V_{mp}}{I_{sc}V_{oc}}$$

$$\eta\equiv\frac{P_{max}}{P_{in}}=\frac{I_{mp}V_{mp}}{P_{in}}$$

Where Pmax is the maximum power point, FF is the fill factor, and η is the efficiency. The fill factor measures the "squareness" of the IV curve.

g. Electrical Output

A solar cell is a p-n junction photodiode. In order to obtain the IV characteristic of the solar cell, the dark current needs to be subtracted from the photogenerated current.

$$I = I_L - I_D$$

The dark current is the current through the solar cell when bias is applied in the dark [10, p. 30].

Graphically, the IV characteristic is obtained in Figure 19.

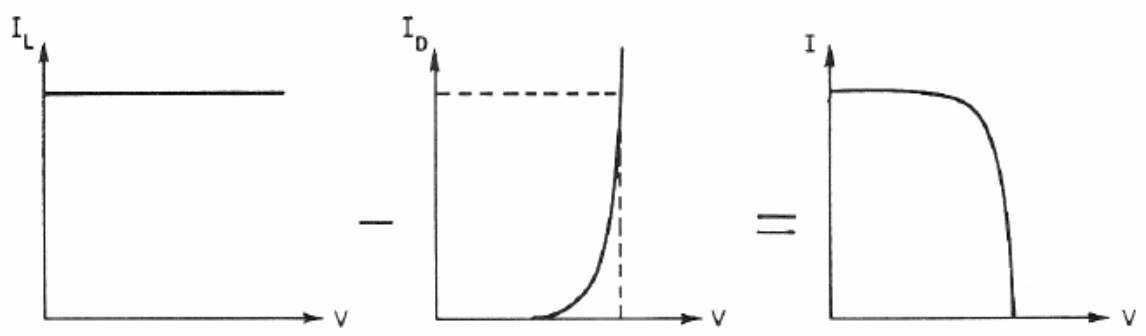

Figure 19. Solar cell IV characteristic (From [21]).

C. CHAPTER CONCLUSIONS

This chapter provided basic information on semiconductors and solar cells. The foundation has been established from the physics stand point. The next step is to cover an introduction to the simulation software.

III. SILVACO ATLAS SIMULATION SOFTWARE

This thesis uses Silvaco Atlas to perform solar cell modeling. Silvaco International produces a suite of software programs that together become a Virtual Wafer Fabrication tool. This chapter introduces Silvaco Atlas and some of its features.

A. VIRTUAL WAFER FAB

Silvaco International provides several software tools to perform process and device simulation. From Figure 20, it can be seen that Silvaco offers powerful simulation software.

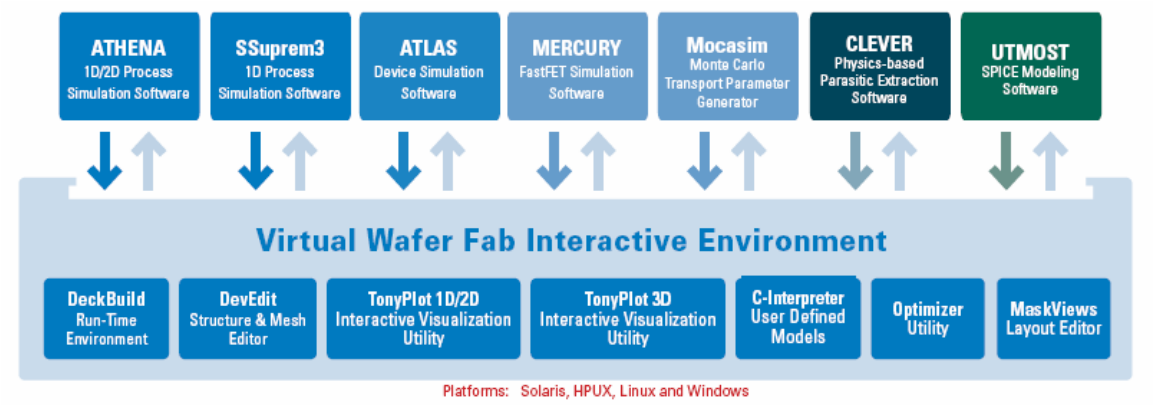

Figure 20. Silvaco's Virtual Wafer Fabrication Environment (From [22]).

In this thesis, Silvaco Atlas was extensively used. The DeckBuild run-time environment received the input files. Within the input files, Silvaco Atlas was called to execute the code. And finally, TonyPlot was used to view the output of the simulation. Additionally, output log files were produced. The data extracted from the log files could then

be displayed using Microsoft Excel or Matlab scripts. Figure 21 shows the inputs and outputs for Silvaco Atlas.

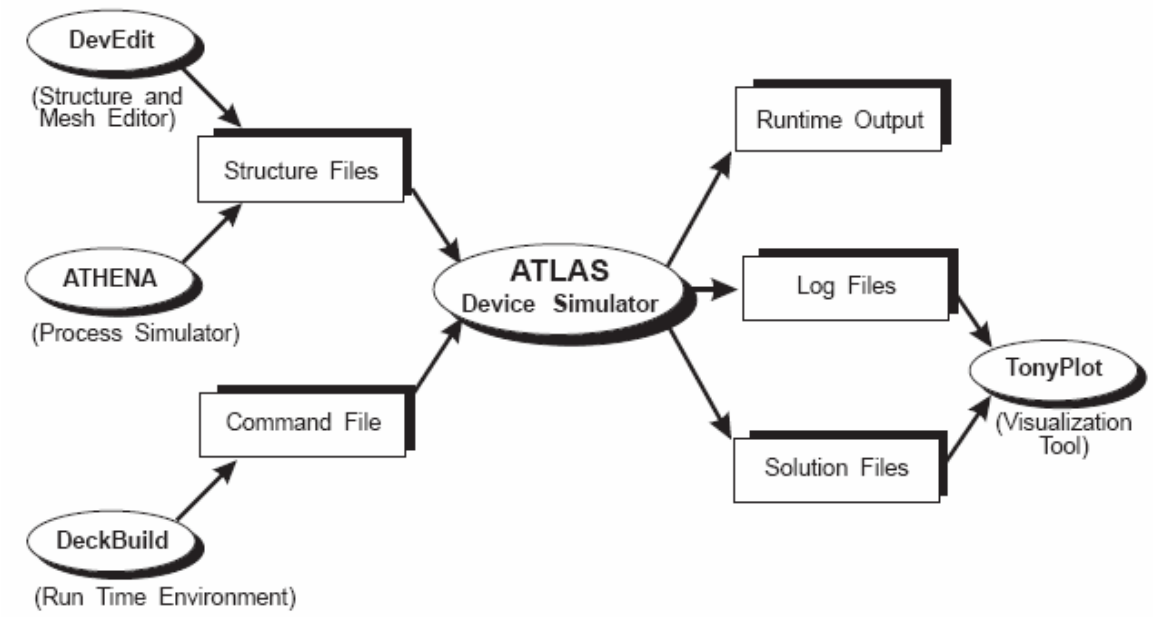

Figure 21. Atlas inputs and outputs (From [23, p. 2-2]).

B. SILVACO ATLAS

Atlas is a software program used to simulate two and three-dimensional semiconductor devices. The physical models include in Atlas are presented in Table 6.

- DC, AC small-signal, and full time-dependency.
- Drift-diffusion transport models.
- Energy balance and Hydrodynamic transport models.
- Lattice heating and heatsinks.
- Graded and abrupt heterojunctions.
- Optoelectronic interactions with general ray tracing.
- Amorphous and polycrystalline materials.
- General circuit environments.
- Stimulated emission and radiation
- Fermi-Dirac and Boltzmann statistics.
- Advanced mobility models.
- Heavy doping effects.
- Full acceptor and donor trap dynamics
- Ohmic, Schottky, and insulating contacts.
- SRH, radiative, Auger, and surface recombination.
- Impact ionization (local and non-local).
- Floating gates.
- Band-to-band and Fowler-Nordheim tunneling.
- Hot carrier injection.
- Quantum transport models
- Thermionic emission currents.

Table 6. Silvaco Atlas physical models (From [23, p. 1-2]).

C. INPUT FILE STRUCTURE

Silvaco Atlas receives input files through DeckBuild. The code entered in the input file calls Atlas to run with the following command:

```
go atlas
```

Following that command, the input file needs to follow a pattern. The command groups are listed in Figure 22.

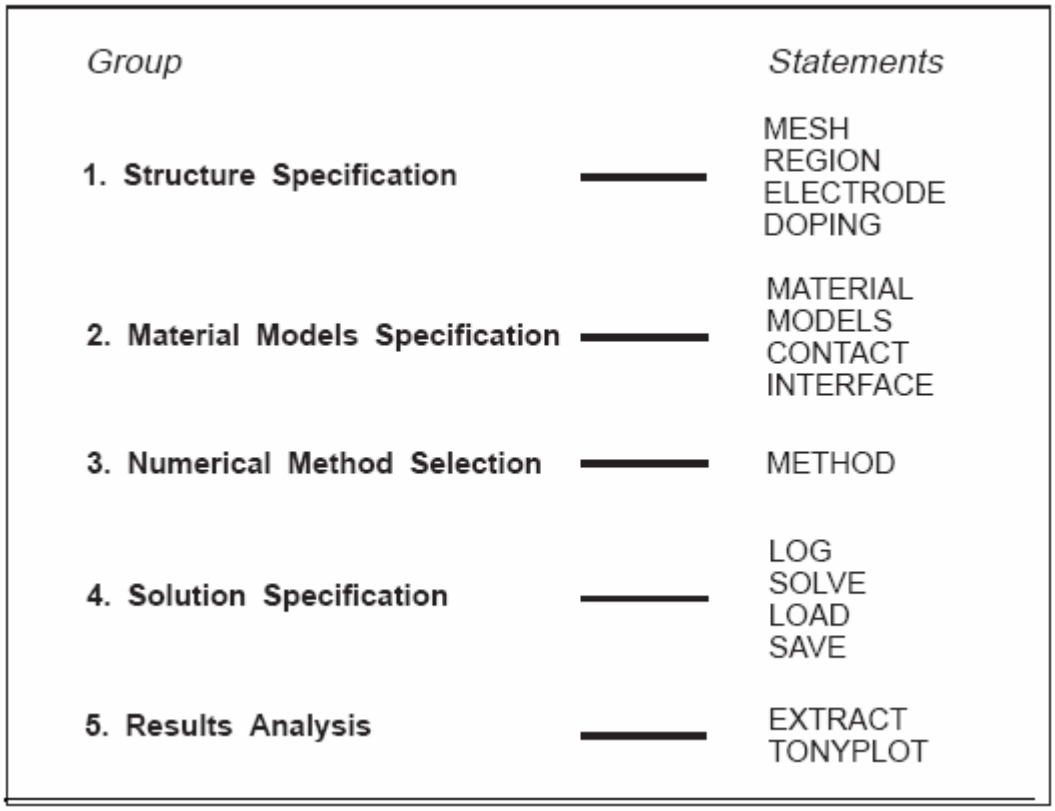

Figure 22. Atlas command groups and primary statements (From [23, p. 2-8]).

Atlas follows the following format for statements and parameters:

<STATEMENT> <PARAMETER>=<VALUE>

The following line of code serves as an example.

```
DOPING UNIFORM N.TYPE CONCENTRATION=1.0e16 REGION=1 \
OUTFILE=my.dop
```

The statement is DOPING. The parameters are UNIFORM, N.TYPE, CONCENTRATION, REGION, and OUTFILE. There are four different type of parameters: real, integer, character, and logical. The back slash (\) serves the purpose of continuing the code in the next line. Parameters, such as UNIFORM, are

logical. Unless a TRUE or FALSE value is assigned, the parameter is assigned the default value. This value can be either TRUE or FALSE. The Silvaco Atlas manual needs to be referenced to identify the default value assigned to specific parameters.

1. Structure Specification

The structure specification is done by defining the mesh, the region, the electrodes and the doping levels.

a. Mesh

The mesh used for this thesis is two-dimensional. Therefore, only x and y parameters are defined. The mesh is a series of horizontal and vertical lines and spacing between them. From Figure 23, the mesh statements are specified.

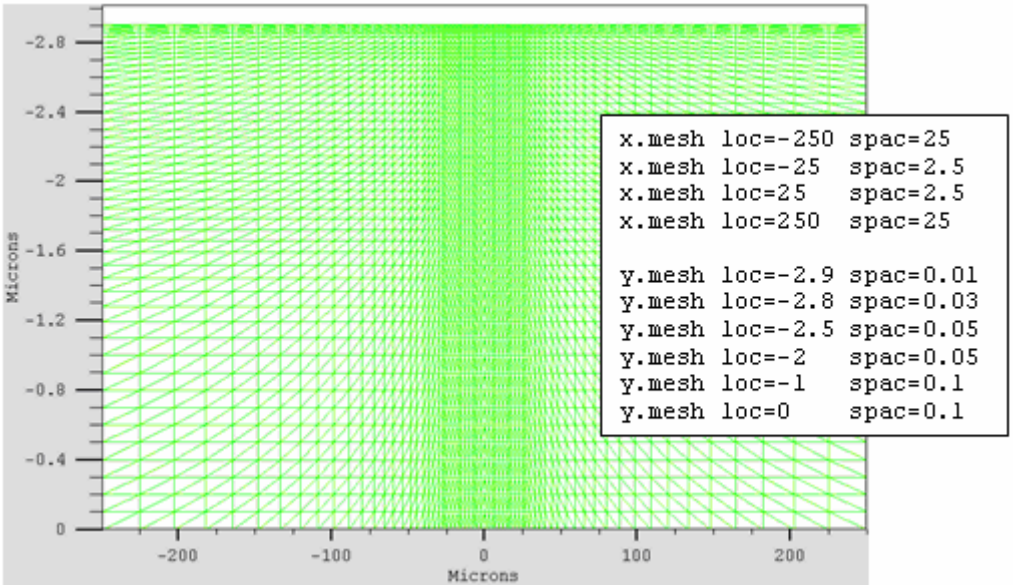

Figure 23. Atlas mesh (From 2, p.18]).

The general format to define the mesh is:

X.MESH LOCATION=<VALUE> SPACING=<VALUE>

Y.MESH LOCATION=<VALUE> SPACING=<VALUE>

For example, the x.mesh starting at -250 microns has spacing of 25 microns. That means it is relatively coarse. The x.mesh becomes finer between -25 and 25 microns with a spacing of 2.5 microns. The y.mesh is similarly defined. For example, at y.mesh of -2.9 microns, the spacing is 0.01 microns. Then at location y.mesh of -2.8 microns, the spacing changes to 0.03 microns. The mesh is coarser at y.mesh location of -1, when the spacing is 0.1.

A coarse or fine mesh determines the accuracy of the simulation. A coarse mesh produces a faster simulation, but less accurate results. A fine mesh produces a slower simulation, but more accurate results. The areas that have a finer mesh, therefore, are of greatest interest in the simulation.

b. Region

After defining the mesh, it is necessary to define the regions. The format to define the regions is as follows:

REGION number=<integer> <material_type> /

<position parameters>

From Figure 24, the code that defines the regions is identified. There are six regions defined. The limits of each region are explicitly identified in the x- and y-axis. The regions must then be given a material.

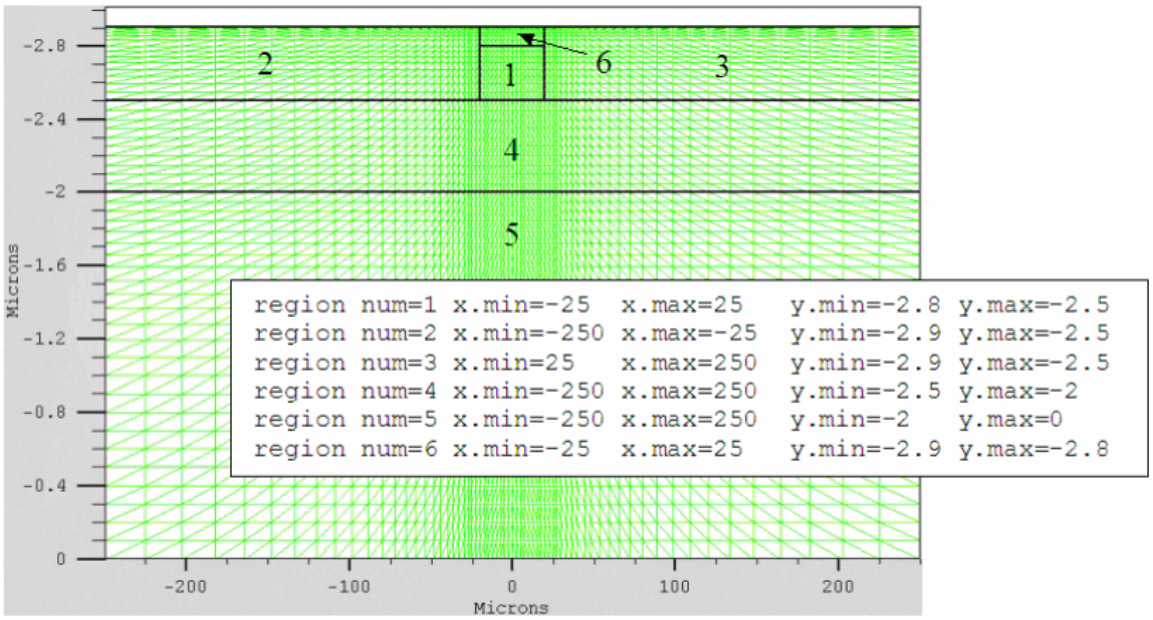

Figure 24. Atlas region (From [2, p. 19]).

From Figure 25, the code defines the material for each region. Note that the color coding identifies the material. The regions have vertical and horizontal lines to mark their boundaries.

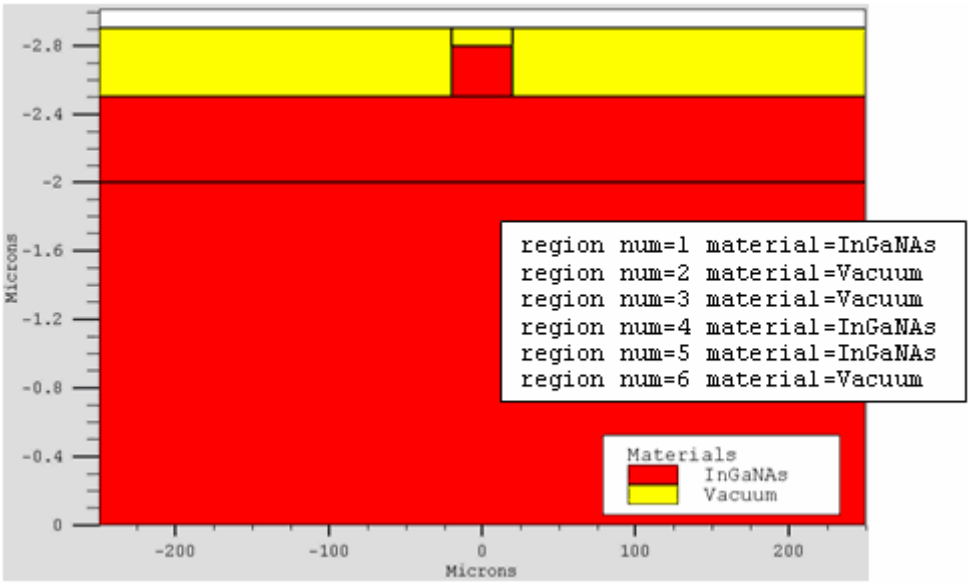

Figure 25. Atlas regions with materials defined (From [2, p. 19]).

c. Electrodes

The next structure specification corresponds to electrodes. Typically, in this simulation the only electrodes defined are the anode and the cathode. However, Silvaco Atlas has a limit of 50 electrodes that can be defined. The format to define electrodes is as follows:

ELECTRODE NAME=<electrode name> <position_parameters>

From Figure 26, the electrode statements are defined for the anode and the cathode. Note that the cathode is defined with gold as the material. The x and y dimensions correspond to region 6 previously defined. Meanwhile, the anode is defined at the bottom of the cell for the entire x-range at y=0.

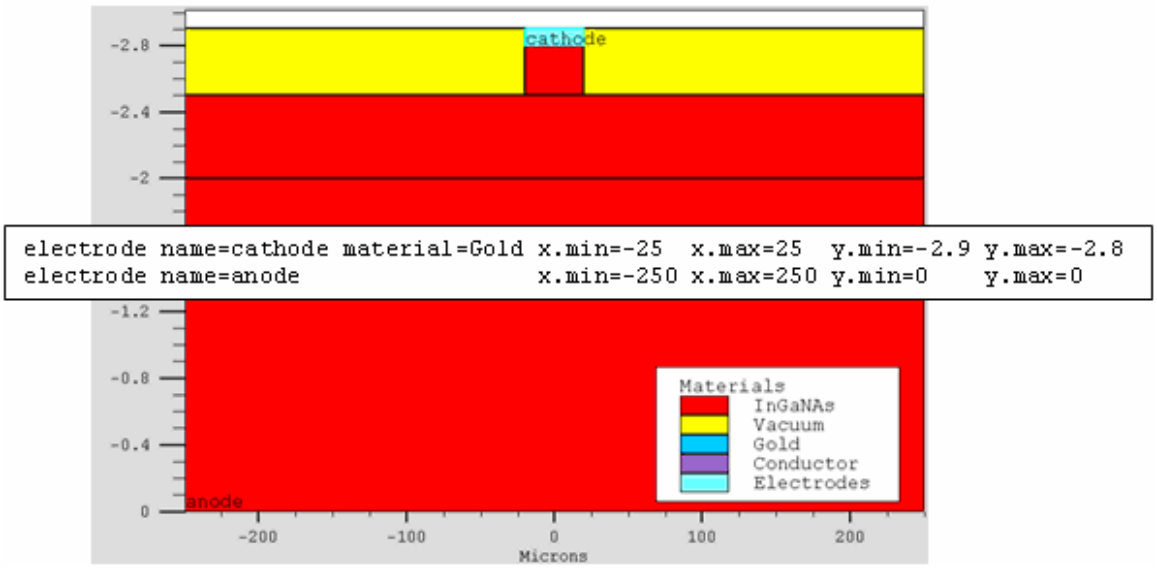

Figure 26. Atlas electrodes (From [2, p. 20]).

d. Doping

The last aspect of structure specification that needs to be defined is doping. The format of the Atlas statement is as follows:

DOPING <distribution type> <dopant_type> /

<position parameters>

From Figure 27, the doping types and the doping levels are defined. Doping can be n-type or p-type. The distribution type can be uniform or Gaussian.

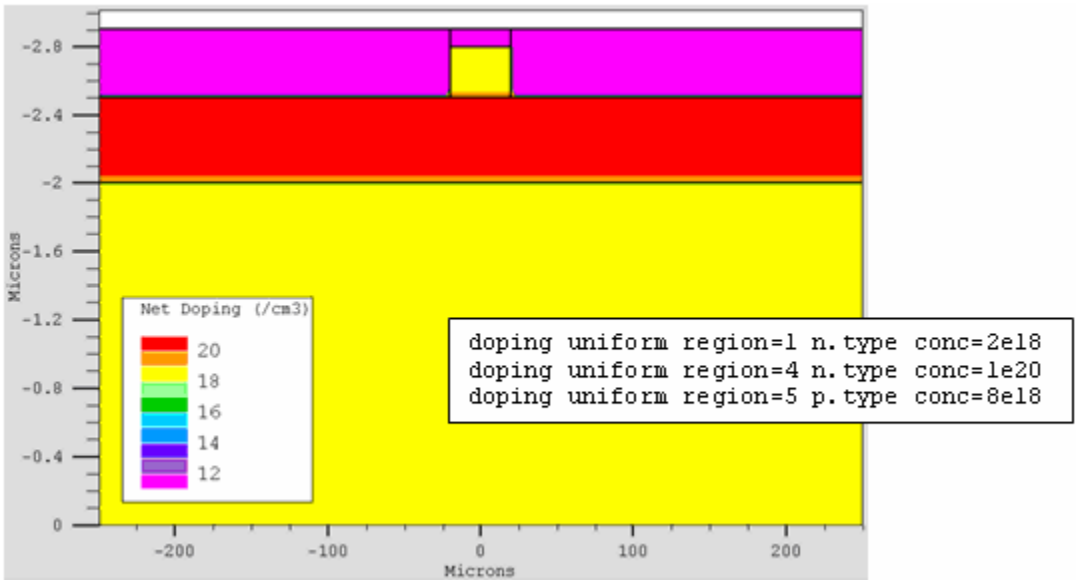

Figure 27. Atlas doping (From [2, p. 21]).

2. Materials Model Specification

After the structure specification, the materials model specification is next. From Figure 28, the materials model specification is broken down into material, models, contact, and interface.

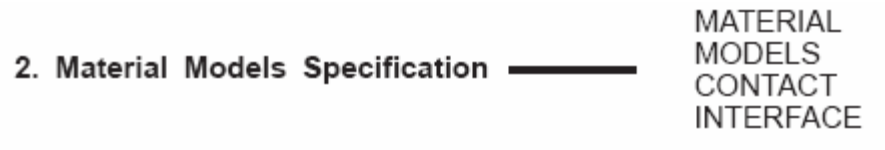

Figure 28. Atlas material models specification (After [23, p. 2-8]).

a. Material

The format for the material statement is as follows:

MATERIAL <localization> <material_definition>

Below are three examples of the material statement:

```
MATERIAL MATERIAL=Silicon EG300=1.1 MUN=1200

MATERIAL REGION=4 TAUN0=3e-7 TAUP0=2e-5

MATERIAL NAME=base NC300=4e18
```

In all examples, when MATERIAL appears first, it is considered the statement. When MATERIAL appears a second time in the first example, it is considered a localization parameter. In the second and third examples, the localization parameters are REGION and NAME, respectively. Various other parameters can be defined with the material statement. Examples of these parameters are the band gap at room temperature (EG300), electron mobility (MUN), electron (TAUN0) and hole (TAUP0) recombination lifetimes, conduction band density at room temperature (NC300), among others.

b. Models

The physical models fall into five categories: mobility, recombination, carrier statistics, impact

ionization, and tunneling. The syntax of the model statement is as follows:

MODELS <model flag> <general parameter> /

<model dependent parameters>

The choice of model depends on the materials chosen for simulation.

The example below activates several models.

MODELS CONMOB FLDMOB SRH

CONMOB is the concentration dependent model. FLDMOB is the parallel electric field dependence model. SRH is the Shockley-Read-Hall model.

c. Contact

Contact determines the attributes of the electrode. The syntax for contact is as follows:

CONTACT NUMBER=<n> |NAME=<ename>|ALL

The following is an example of the contact statement.

CONTACT NAME=anode current

d. Interface

The semiconductor or insulator boundaries are determined with the interface statement. The syntax is as follows:

INTERFACE [<parameters>]

The following example shows the usage of the interface statement.

```
INTERFACE X.MIN=-4 X.MAX=4 Y.MIN=-0.5 Y.MAX=4 \
QF=1e10 S.N=1e4 S.P=1e4
```

The max and min values determine the boundaries. The QF value specifies the fixed oxide charge density (cm^{-2}). The S.N value specifies the electron surface recombination velocity. S.P is similar to S.N, but for holes.

3. Numerical Method Selection

After the materials model specification, the numerical method selection must be specified. From Figure 29, the only statement that applies to numerical method selection is method.

Figure 29. Atlas numerical method selection (After [23, p. 2-8]).

There are various numerical methods to calculate solutions to semiconductor device problems. There are three types of solution techniques used in Silvaco Atlas:

- decoupled (GUMMEL)
- fully coupled (NEWTON)
- BLOCK

The GUMMEL method solves for each unknowns by keeping all other unknowns constant. The process is repeated until there is a stable solution. The NEWTON method solves all

unknowns simultaneously. The BLOCK method solves some equations with the GUMMEL method and some with the NEWTON method.

The GUMMEL method is used for a system of equations that are weakly coupled and there is linear convergence. The NEWTON method is used when equations are strongly coupled and there is quadratic convergence.

The following example shows the use of the method statement.

METHOD GUMMEL NEWTON

In this example, the equations are solved with the GUMMEL method. If convergence is not achieved, then the equations are solved using the NEWTON method.

4. Solution Specification

After completing the numerical method selection, the solution specification is next. Solution specification is broken down into log, solve, load, and save statements, as shown in Figure 30.

Figure 30. Atlas solution specification (After [23, p. 2-8]).

a. Log

LOG saves all terminal characteristics to a file. DC, transient, or AC data generated by a SOLVE statement after a LOG statement is saved.

The following shows an example of the LOG statement.

```
LOG OUTFILE=myoutputfile.log
```

The example saves the current-voltage information into myoutputfile.log.

b. Solve

The SOLVE statement follows the LOG statement. SOLVE performs a solution for one or more bias points. The following is an example of the SOLVE statement.

```
SOLVE B1=10 B3=5 BEAM=1 SS.PHOT SS.LIGHT=0.01 \
MULT.F FREQUENCY=1e3 FSTEP=10 NFSTEP=6
```

B1 and B3 specify the optical spot power associated with the optical beam numbers 1 and 3, respectively. The beam number is an integer between 1 and 10. BEAM is the beam number of the optical beam during AC photogeneration analysis. SS.PHOT is the small signal AC analysis. SS.LIGHT is the intensity of the small signal part of the optical beam during signal AC photogeneration analysis. MULT.F is the frequency to be multiplied by FSTEP. NFSTEPS is the number of times that the frequency is incremented by FSTEP.

c. Load and Save

The LOAD statement enters previous solutions from files as initial guess to other bias points. The SAVE statement enters all node point information into an output file.

The following are examples of LOAD and SAVE statements.

SAVE OUTF=SOL.STR

In this case, SOL.STR has information saved after a SOLVE statement. Then, in a different simulation, SOL.STR can be loaded as follows:

LOAD INFILE=SOL.STR

5. Results Analysis

Once a solution has been found for a semiconductor device problem, the information can be displayed graphically with TonyPlot. Additionally, device parameters can be extracted with the EXTRACT statement, as shown in Figure 31.

Figure 31. Atlas results analysis (After [23, p. 2-8]).

In the example below, the EXTRACT statement obtains the current and voltage characteristics of a solar cell. This information is saved into the IVcurve.dat file. Then, TonyPlot plots the information in the IVcurve.dat file.

```
EXTRACT NAME="iv" curve(v."anode", I."cathode") /
OUTFILE="IVcurve.dat"

TONYPLOT IVcurve.dat
```

Figure 32 shows the sample IV curve plotted by TonyPlot.

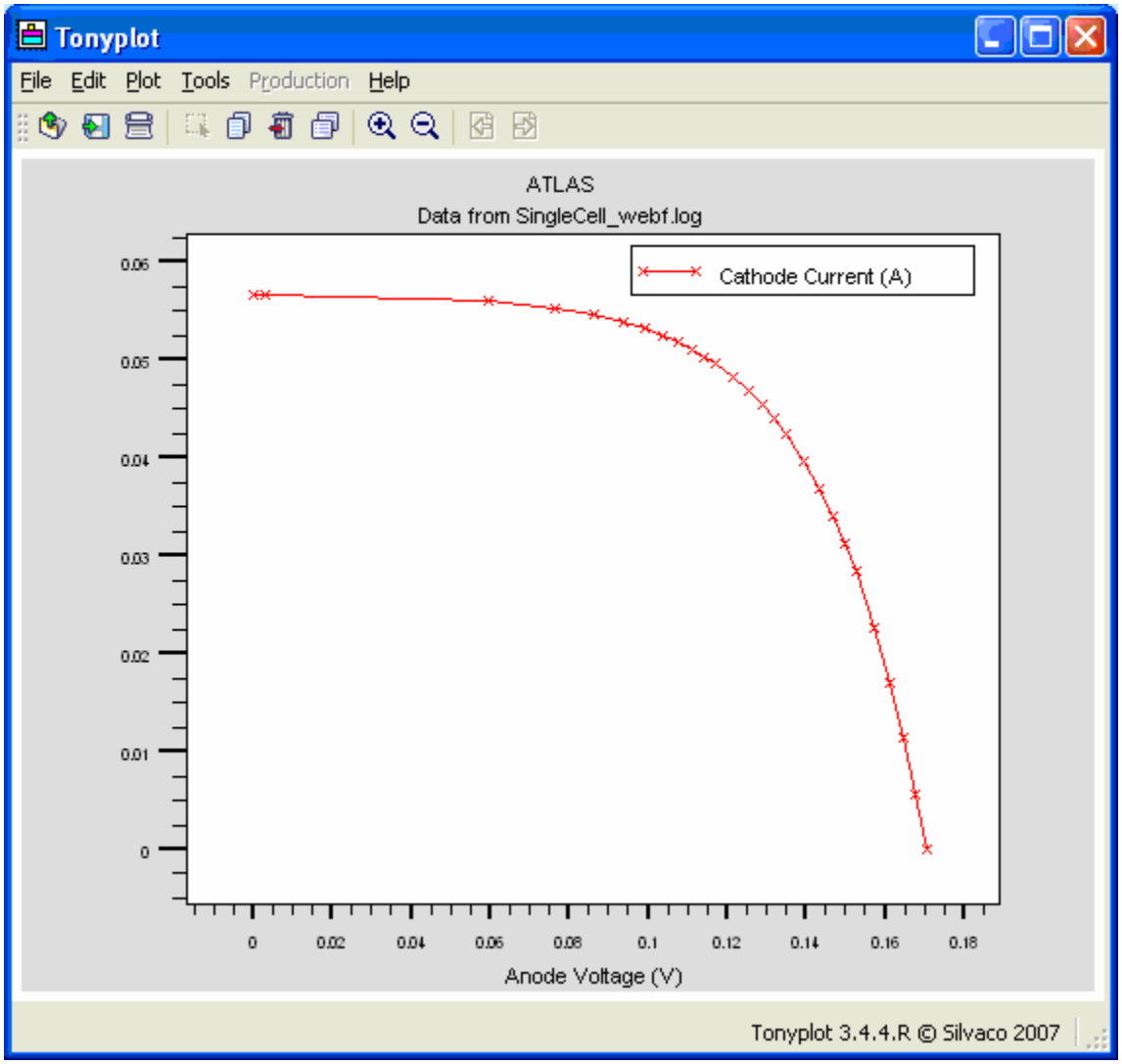

Figure 32. Sample TonyPlot IV curve.

D. CONCLUSION

This chapter presented an introduction to Silvaco Atlas, the structure of the input files, and some of its statements. With these basic tools, the next chapter introduces some basic information on wurtzite Indium Gallium Nitride before proceeding to the thesis simulation.

IV. INDIUM GALLIUM NITRIDE

A. A FULL SPECTRUM PHOTOVOLTAIC MATERIAL

Prior to 2001, it was thought that wurtzite Indium Nitride had a band gap of approximately 1.9 eV. In 2001, it was discovered that Indium Nitride had a much smaller band gap. Davydov, et al., concluded in [24] that Indium Nitride had a band gap of approximately 0.9 eV. Additionally, Davydov, et al., presented in [25] that wurtzite Indium Gallium Nitride band gaps in the range x=0.36 to x=1 supported findings in [24]. The band gaps for Indium Gallium Nitride, with Indium Nitride concentrations ranging from 0.0 to 1.0 are presented in Figure 33.

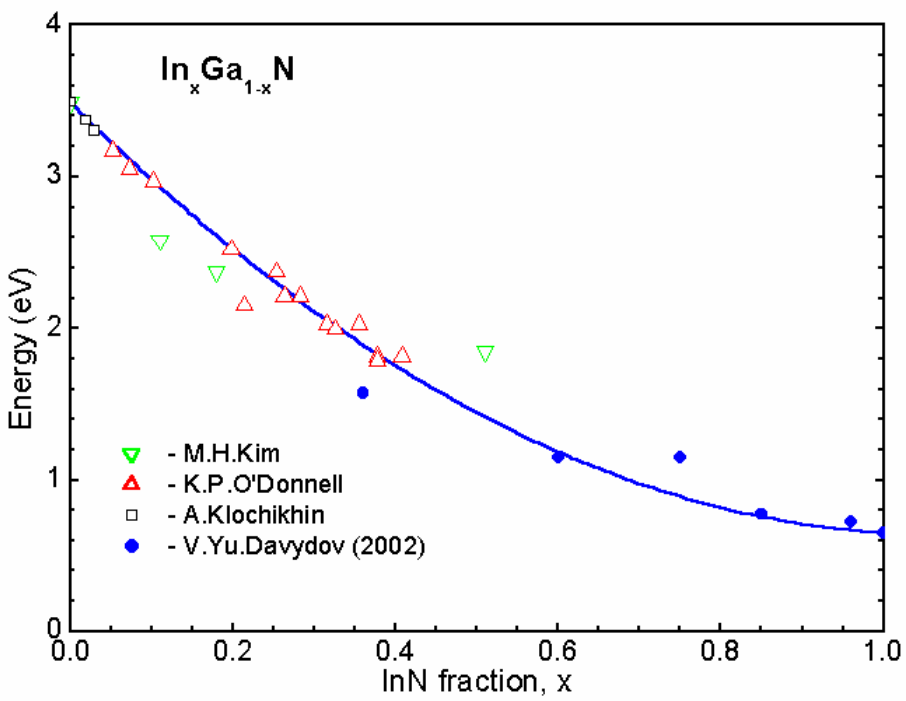

Figure 33. InGaN band gap as a function of In composition (After [25]).

Later on, research conducted at Lawrence Berkeley National Laboratory presented that the Indium Nitride fundamental band gap was approximately 0.77 eV at room temperature. Since Gallium Nitride has a band gap of approximately 3.4 eV at room temperature, then Indium Gallium Nitride can have a band gap ranging from 0.77 eV to 3.4 eV by changing the percent composition of Indium and Gallium within Indium Gallium Nitride. Figure 34 confirms that Indium Gallium Nitride follows the pattern of ranging from 0.77 eV to 3.4 eV.

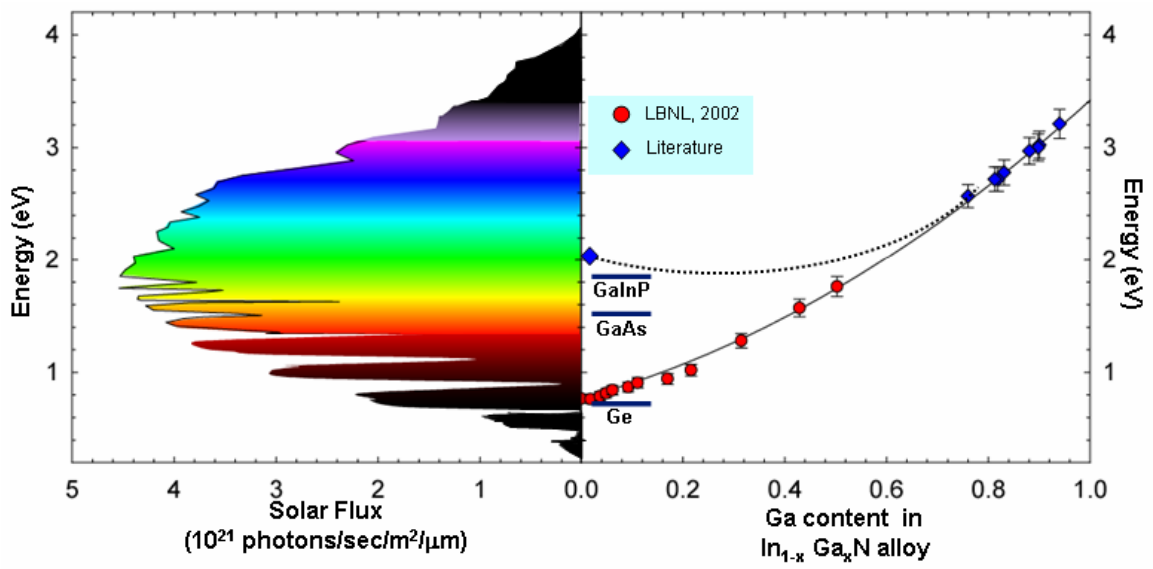

Figure 34. InGaN band gap and solar spectrum comparison (After [26]).

Figure 34 also presents the solar spectrum on the left-hand side. Therefore, it is clear that the visible spectrum has a near-perfect match with the Indium Gallium Nitride range of band gaps.

It should be noted that research conducted in [27] presents a Indium Nitride band gap of 1.7±0.2 eV. It is stated in [27], “These investigations clarify that a band

transition around 1.7 eV does exist in wurtzite InN although in this energy range optical material responses are hardly ever found. If the 1.7 eV band transition is indeed the fundamental bandgap in InN at room temperature it is concluded that defect bands, grain boundaries, dislocations and/or the very conductive surface are contributing to the lower energy optical responses in InN. The identification of the various defects in InN will be subject of future investigations."

In follow up research, [28] explains the possible reason for the higher Indium Nitride band gap: "Owing to InN's exceptional propensity for n-type activity, in many instances the larger apparent values of the band gap can be attributed to the Burstein–Moss shift of the optical absorption edge resulting from the occupation of conduction band states by free electrons."

Figure 35 shows evidence that the fundamental band gap of indium nitride is approximately 0.7 eV, and not near 2 eV. The optical absorption (blue curve) has an onset at approximately 0.8 eV. There is no change in absorption around the 2 eV range. The photo luminescence (red curve) shows a peak at the band edge of approximately 0.8 eV. Finally, the photo-modulated reflectance (green curve) presents a transition close to 0.8 eV. These three curves support a band gap for indium nitride of approximately 0.8 eV. The 1.9-2.0 eV band gap is not evident in Figure 35.

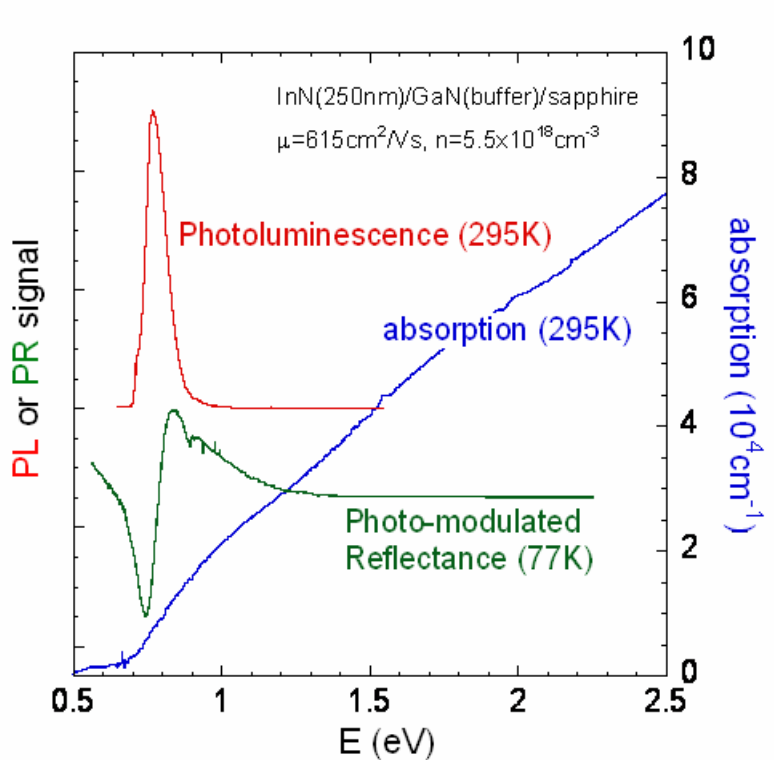

Figure 35. Evidence of 0.7 eV band gap for indium nitride (From [29]).

The controversy about indium nitride's fundamental band gap is not the subject of this thesis. This research proceeded accepting the fundamental band gap of 0.77 eV for indium nitride.

According to [30], the following formula provides an approximation of Indium Gallium Nitride band gap:

$$E_G(x) = 3.42x + 0.77(1-x) - 1.43x(1-x)$$

Where E_G is the InGaN band gap, 3.42 eV is the GaN band gap, 0.77 eV is the InN band gap, 1.43 eV is the bowing parameter b, x is the Ga concentration, and (1-x) is the In concentration.

When plotting the band gap formula for InGaN using a Matlab script, the Figure 36 is obtained.

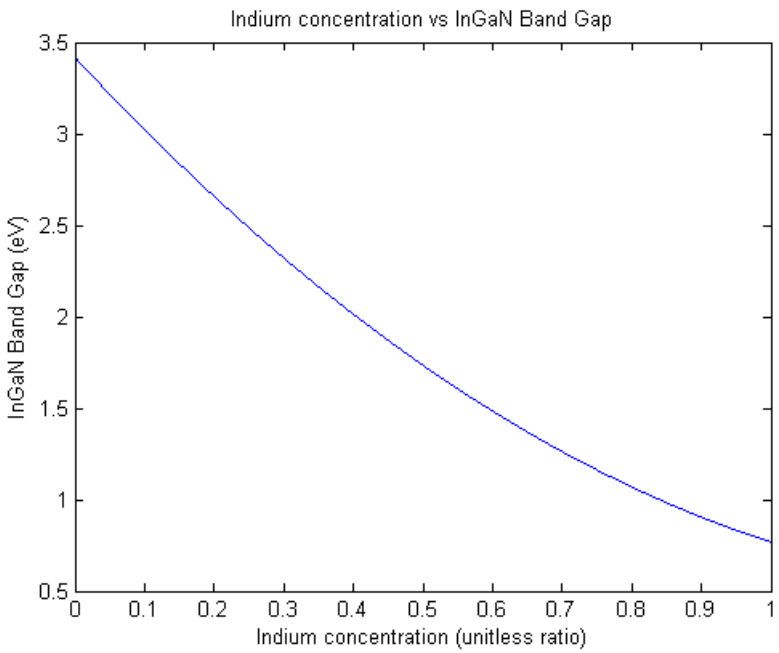

Figure 36. InGaN band gap as a function of In concentration.

The band gaps used in the Silvaco Atlas simulations were found by modifying the Matlab script for Figure 35.

B. RADIATION-HARD SEMICONDUCTOR MATERIAL

Radiation-hard materials are essential for space applications. When compared to other Gallium Arsenide and Indium Gallium Phosphide, Indium Gallium Nitride is able to withstand a greater amount of radiation. According to [31], InGaN "retains its optoelectronic properties at radiation damage doses at least two orders of magnitude higher than the damage thresholds of the materials (GaAs and GaInP) currently used in high efficiency MJ cells". Radiation levels in [31] were 1 MeV electron, 2 MeV proton, and 2 MeV alpha particle irradiation.

This indicates that InGaN is not only potentially a high-efficiency photovoltaic material, but it is also able to withstand the harsh space environment.

C. INDIUM GALLIUM NITRIDE CHALLENGES

There are some significant issues that currently prevent InGaN from being used as photovoltaic material. As of this writing, no PN junction has been built. The PN junction is essential to create photodiodes. Indium Nitride has the highest electron affinity among all semiconductors [32]. Hence, Indium Nitride has a tendency to be n-type. It is much more difficult to build p-type material with Indium Nitride. However, evidence of p-type doping in Indium Nitride and Indium Gallium Nitride has been reported in [33] using Magnesium. This is a step in the right direction. Further progress in this area dictates the creation of Indium Gallium Nitride PN junctions.

Having reviewed the characteristics of Indium Gallium Nitride, the next chapter covers the simulation of Indium Gallium Nitride using Silvaco Atlas.

V. SIMULATION OF INDIUM GALLIUM NITRIDE IN SILVACO ATLAS

One of the primary motivations behind this research was to find a way to make solar cells significantly more efficient. When researching high-efficiency solar cells, the improvements were typically incremental over previous results. Solar cells were first designed as single-junction. The most popular photovoltaic material has been Silicon due to its abundance and relatively low cost. The maximum efficiency of polycrystalline Silicon is approximately 19.8%. Commercial silicon solar cells have a maximum efficiency of approximately 13%. Improvements in efficiency can be obtained in single-junction solar cells by using Gallium Arsenide. Monocrystalline Gallium Arsenide has a maximum efficiency of approximately 25.1% [10, p. 195].

By designing dual-junction solar cells, the efficiency can again be improved. A dual-junction cell with Gallium Phosphide as the top junction and Gallium Arsenide as the bottom cell can have an efficiency of 30.3% [10, p 302].

Increasing the number of junctions makes the cells more complex in design and the gains begin to diminish. Triple-junction cells have efficiencies of approximately 31%. Quad-junction cells have efficiencies of approximately 33%. It is expected that five- and six-junction solar cells can have efficiencies of approximately 35% [36].

This simulation uses Indium Gallium Nitride as photovoltaic material in a simulation. With its full-spectrum characteristics, the efficiency of Indium Gallium Nitride has the potential to surpass previous results.

A. SINGLE-JUNCTION SOLAR CELL

Figure 37 shows a graphical representation of the single junction solar cell. The thickness of the emitter is 0.01 μm and the doping is $1x10^{16}/cm^3$. The thickness of the base is 3 μm and the doping is $1x10^{16}/cm^3$.

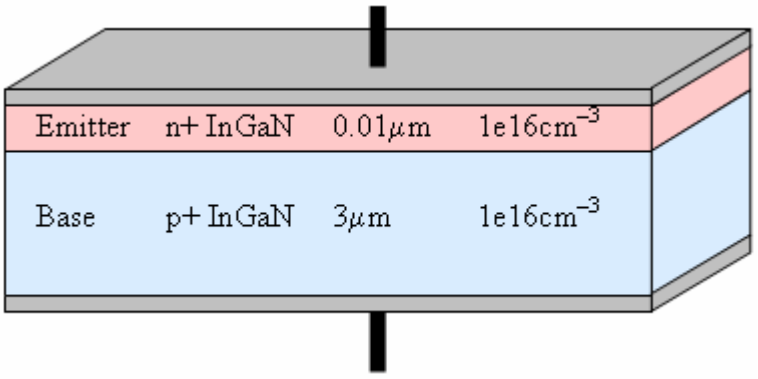

Figure 37. Simple single-junction InGaN solar cell.

The first step is to develop single junction solar cells. Optical data in the form of dielectric constants was found in [34] for $In_{0.20}Ga_{0.80}N$. This corresponds to a calculated band gap of 2.66 eV. Additional optical data was found in [35] for $In_{0.57}Ga_{0.43}N$ (calculated Eg=1.60 eV), $In_{0.68}Ga_{0.32}N$ (calculated Eg=1.31 eV), and $In_{0.78}Ga_{0.22}N$ (calculated Eg=1.1 eV). The dielectric constants were then converted to index of refraction (n) and extinction coefficient (k) using a Matlab script (Appendix B). The band gap and the optical data were entered into the input deck. The simulation ran in Silvaco Atlas. From the log file, the current and voltage data was extracted.

In the single-junction case, each of the cells had AM0 as the input spectrum. Figure 38 shows the IV curves of four single-junction solar cells. The IV curve pattern corresponds to empirical findings of other multijunction

solar cells. Typically, the cell with the highest voltage has the lowest current. The cell with the lowest voltage has the highest current.

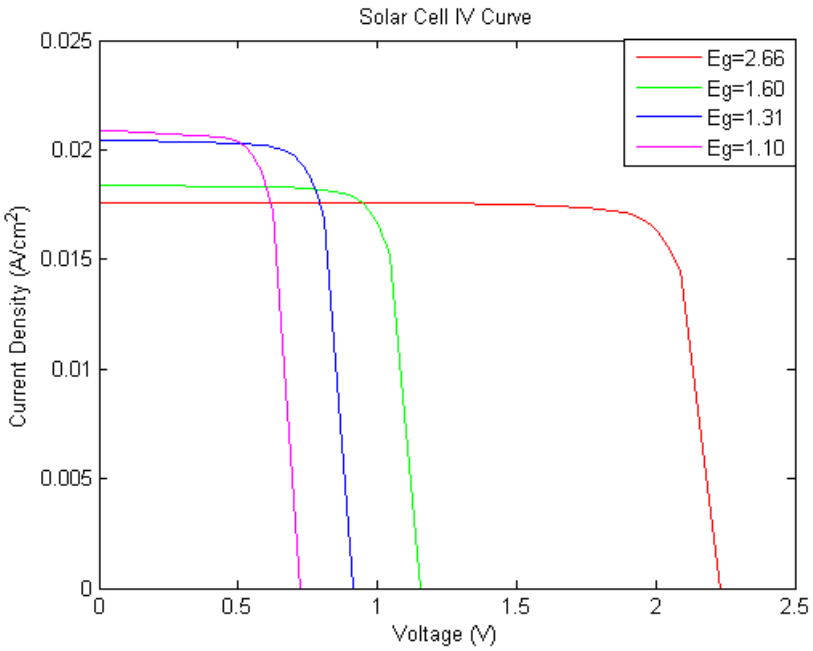

Figure 38. Four single-junction IV curves.

Table 7 shows Isc, Voc, fill factor, and efficiency of the single-junction solar cells presented in Fig. 36.

Material	Isc (mA/cm^2)	Voc (V)	Fill factor	Efficiency
$In_{0.20}Ga_{0.80}N$	17.613	2.23	83.72%	24.32%
$In_{0.57}Ga_{0.43}N$	18.395	1.15	78.80%	12.35%
$In_{0.68}Ga_{0.32}N$	20.453	0.91	76.38%	10.52%
$In_{0.78}Ga_{0.22}N$	20.848	0.72	73.73%	08.19%

Table 7. Efficiencies of four single-junction InGaN cells.

The efficiencies shown in Table 7 indicate that a high-efficiency, single-junction cell with $In_{0.20}Ga_{0.80}N$ has good prospects. A 24.32% efficiency compares favorably to the single-junction Gallium Arsenide efficiency of 25.1%. The InGaN cells simulated can be optimized by changing the thickness of the junction and changing the doping levels. Adding a window, a back surface field (BSF) and a buffer can also help in improving the efficiency results. These improvements can be the subject of future research.

B. DUAL-JUNCTION SOLAR CELL

Figure 39 shows a graphical representation of a dual-junction InGaN solar cell. The thicknesses and doping levels remain identical to the single-junction case.

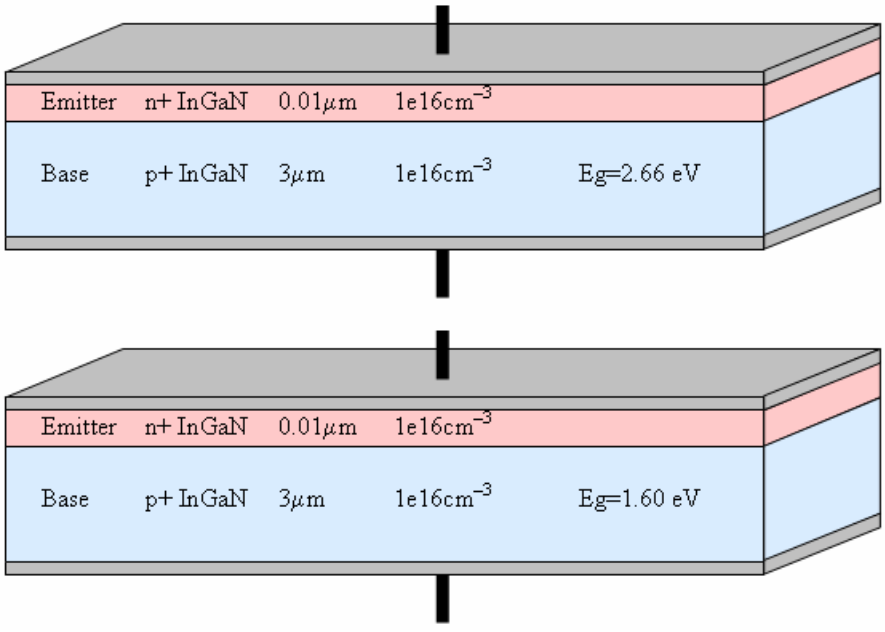

Figure 39. Simple dual-junction InGaN solar cell.

From the discussion in the single-junction solar cell section, it should be clear that the best combination of InGaN band gaps is 2.66 eV and 1.60 eV, since they have the

highest efficiencies. It should be noted that for this simulation, the AM0 spectrum was provided for the top junction $In_{0.20}Ga_{0.80}N$ (Eg=2.66 eV). The bottom junction $In_{0.57}Ga_{0.43}N$ (Eg=1.60 eV) received the AM0 spectrum minus the spectrum absorbed by the top cell.

Figure 40 shows the IV curves of the dual-junction solar cell. Note that compared to Figure 38, the IV curve of Eg=2.66 eV stayed the same, while the IV curve of Eg=1.60 eV had a current drop. This current decrease was expected because the input spectrum was diminished by the top cell.

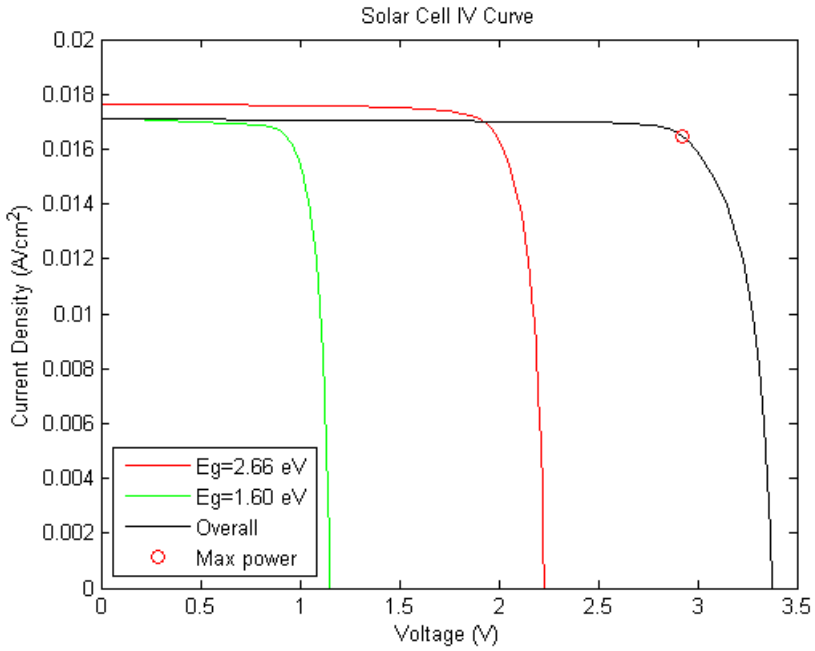

Figure 40. Dual-junction InGaN solar cell IV curve.

Since the junctions are in series, the overall IV curve is limited in its current level by the IV curve with the lowest current. The voltages are added accordingly.

Table 8 shows the efficiency of the dual-junction solar cell.

Material	Isc (mA/cm^2)	Voc (V)	Fill factor	Efficiency
$In_{0.20}Ga_{0.80}N$ $In_{0.57}Ga_{0.43}N$ Dual junction	17.11	3.38	83.25%	35.58%

Table 8. Dual-junction InGaN efficiency.

There is a significant increase in efficiency from single-junction (24.32%) to dual junction (35.58%) InGaN solar cells. This improvement alone should be enough to continue to pursue the development of InGaN solar cells.

Searching for further improvements, three- and four-junction solar cells are examined next.

C. THREE-JUNCTION SOLAR CELL

Figure 41 shows a graphical representation of a three-junction InGaN solar cell. Thicknesses and doping levels stayed the same as the single- and dual-junction cases. From the single-junction solar cell discussion, the three most efficient cells were selected (Eg=2.66 eV, Eg=1.60 eV, Eg=1.31 eV). The top cell $In_{0.20}Ga_{0.80}N$ (Eg=2.66 eV) received the AM0 spectrum. The cell $In_{0.57}Ga_{0.43}N$ (Eg=1.60 eV) received the AM0 spectrum minus the spectrum absorbed by the top cell. The cell $In_{0.68}Ga_{0.32}N$ (Eg=1.31 eV) received the AM0 spectrum minus the spectrum absorbed by the top two cells.

Figure 42 shows the IV curve of the three-junction solar cell. Note that the current level of the top two cells is identical to the dual-junction case. However, the current

level of the bottom cell is lower than the single junction case for the same concentration. Similarly to the dual-junction case, the current of the overall IV curve is limited by the individual junction with the lowest IV curve. The voltages are added accordingly, since the three junctions are in series.

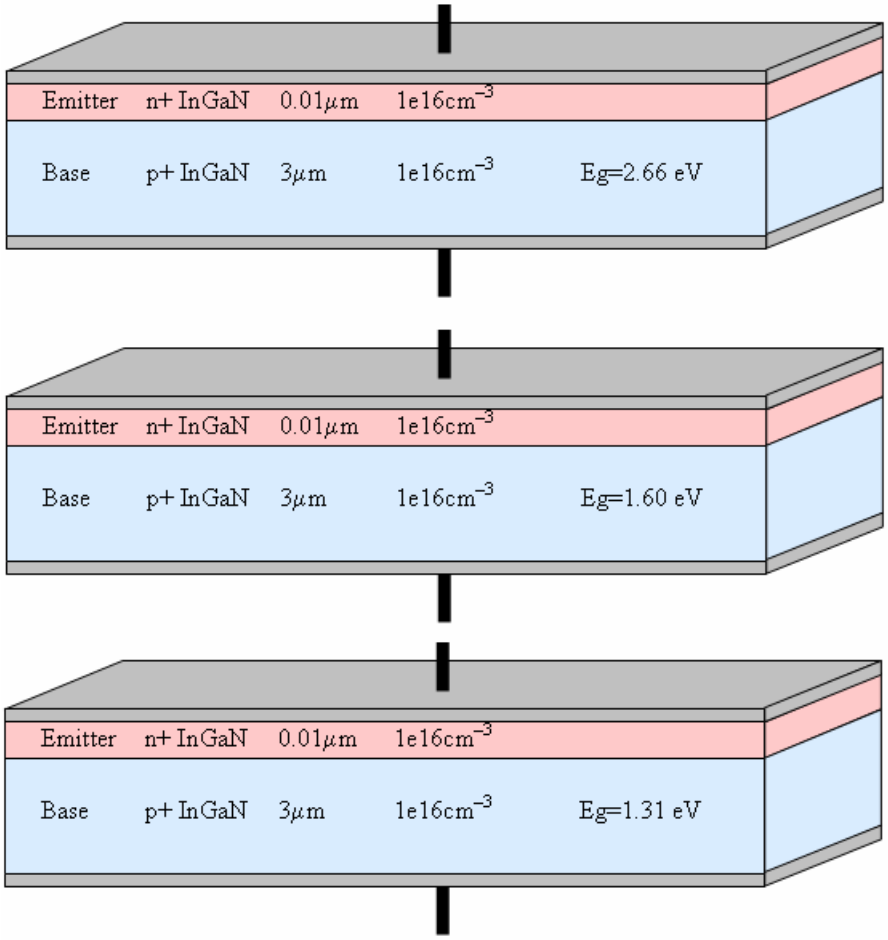

Figure 41. Simple three-junction InGaN solar cell.

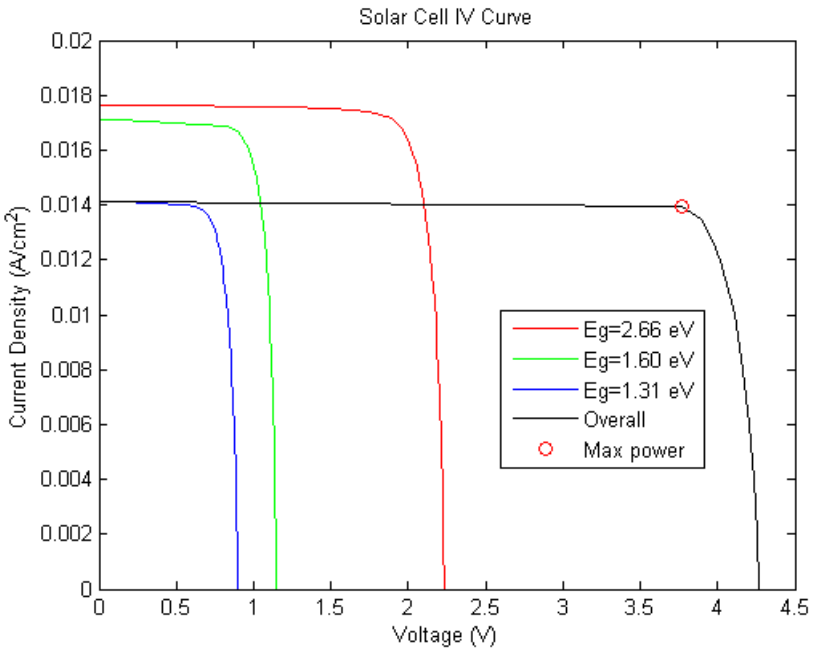

Figure 42. Three-junction InGaN solar cell IV curve.

Table 9 shows the efficiency of the three-junction InGaN solar cell.

Material	Isc (mA/cm^2)	Voc (V)	Fill factor	Efficiency
$In_{0.20}Ga_{0.80}N$ $In_{0.57}Ga_{0.43}N$ $In_{0.68}Ga_{0.32}N$ Three junction	14.12	4.27	87.23%	38.90%

Table 9. Three-junction InGaN efficiency

The increase in efficiency from dual-junction to three-junction is 35.58% to 38.90%. The modest increase in efficiency can be attributed to the drop in Isc from 17.11

mA/cm^2 to 14.12 mA/cm^2. However, the increase in Voc from 3.38 V to 4.27 ensured that the efficiency would increase.

The last case to be examined is the quad-junction InGaN solar cell.

D. QUAD-JUNCTION SOLAR CELL

Figure 43 shows a graphical representation of a quad-junction InGaN solar cell. Thicknesses and doping levels remained the same as the single-, dual-, and three-junction cases. Spectrum input followed the pattern of the dual- and three-junction cases. As expected, the current dropped for all cases where AM0 had been reduced by the top cells.

Figure 44 shows the IV curve for a quad-junction InGaN solar cell. Note that the IV-curves for the top three cells are identical to the three-junction case. The bottom cell has a lower current level compared to the single junction case.

Table 10 shows the efficiency of the quad-junction InGaN solar cell.

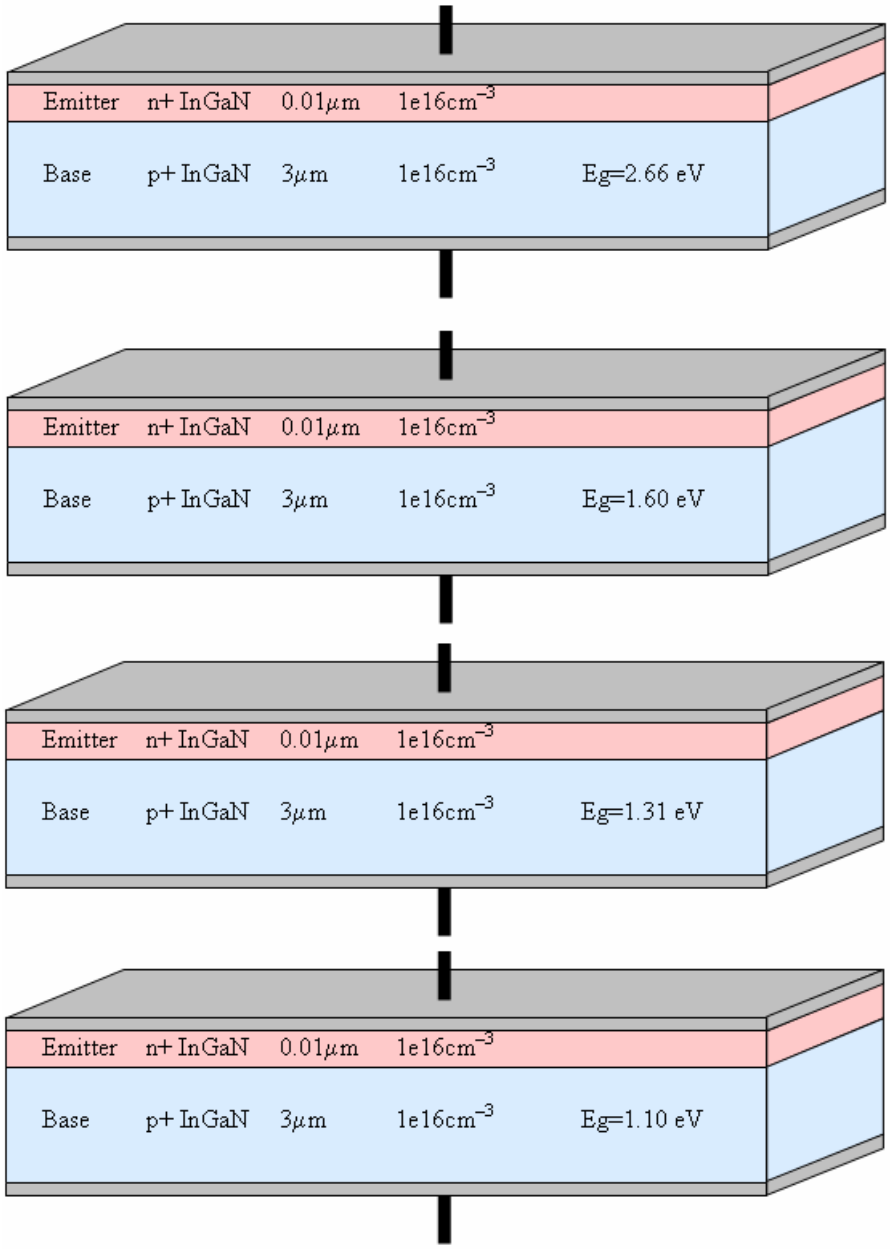

Figure 43. Simple quad-junction InGaN solar cell

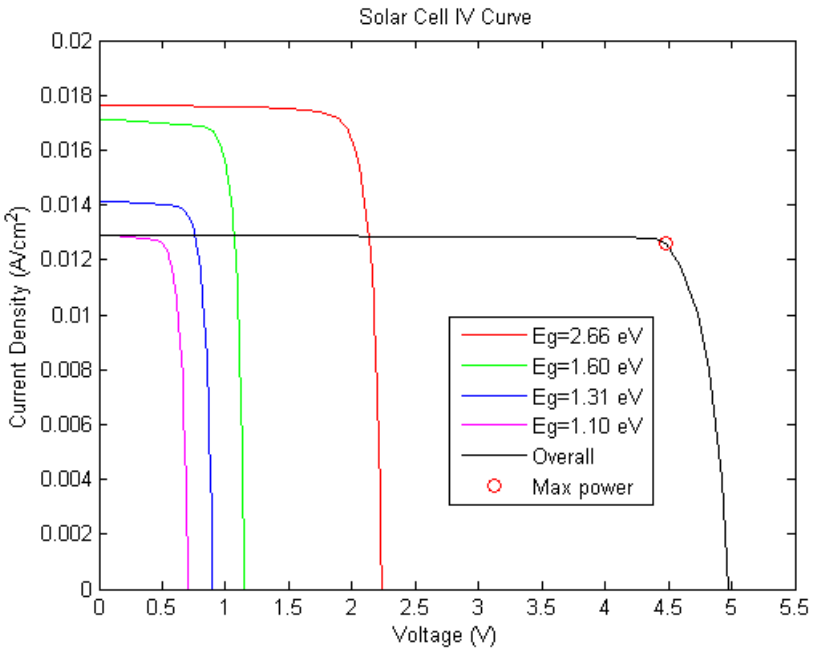

Figure 44. Quad-junction InGaN solar cell IV curve

Material	Isc (mA/cm^2)	Voc (V)	Fill factor	Efficiency
$In_{0.20}Ga_{0.80}N$ $In_{0.57}Ga_{0.43}N$ $In_{0.68}Ga_{0.32}N$ $In_{0.78}Ga_{0.22}N$ Quad-junction	12.88	4.98	87.86%	41.69%

Table 10. Quad junction InGaN efficiency

For completeness, efficiency calculations are provided below for the quad-junction case. These calculations were performed with the help of a Matlab script.

$$P_{max}=I_{mp}V_{mp}=(0.0126\frac{A}{cm^2})(4.4736\ V)=0.0564\frac{W}{cm^2}$$

$$FF=\frac{P_{max}}{I_{sc}V_{oc}}=\frac{I_{mp}V_{mp}}{I_{sc}V_{oc}}=\frac{0.0564\frac{W}{cm^2}}{(0.0129\frac{A}{cm^2})(4.9793V)}=87.86\%$$

$$\eta\equiv\frac{P_{max}}{P_{in}}=\frac{I_{mp}V_{mp}}{P_{in}}=\frac{0.0564\frac{W}{cm^2}}{0.1353\frac{W}{cm^2}}=0.4169=41.69\%$$

In order to get a perspective on how this result compares to actual solar cells in production, Figure 45 is presented.

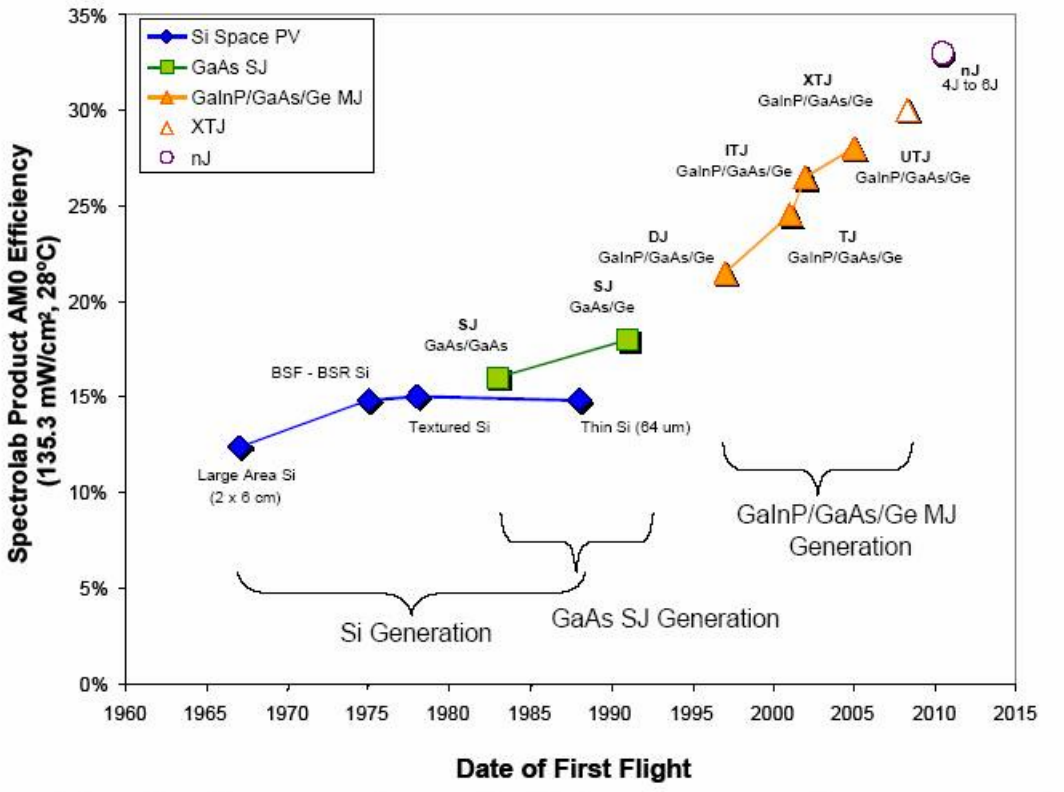

Figure 45. Spectrolab's solar cell efficiencies (From [34]).

The label nJ stands for new generation four to six-junction cells. XTJ is a designation for a triple junction cell. UTJ stands for Ultra Triple Junction. ITJ means Improved Triple Junction. TJ is Triple Junction. DJ is Dual Junction. SJ is single junction.

Figure 45 shows the efficiency progression of a leading solar cell manufacturer (Spectrolab). The first step consists of single junction silicon solar cells. These cells were in production from the mid-1960s until the early 1990s. Their efficiency was close to 15%. The next step consisted of single junction gallium arsenide solar cells. These cells had efficiencies between 15% and 20%. In the mid-1990s, dual junction solar cells appeared. Efficiencies were slightly above 20%. Triple junction cells appeared in the early 2000s with efficiencies nearing 30%. The projections are to produce quad-junction solar cells within the next decade with efficiencies just under 35%.

Further comparisons can be made with another simulation. Modeling in [5] used physics equations to calculate Isc and Voc. The input spectrum used in that simulation was AM1.5 instead of AM0. The InGaN band gap formula used was from [37]. This thesis used the band gap formula from [30]. Figure 46 shows a comparison of the two formulas. Both formulas seek to duplicate findings from actual band gap measurements. Therefore, both formulas are approximations only.

The simulation from [5] obtained the results presented in Table 11. The highest efficiency obtained in that simulation is 40.346% with a six-junction InGaN solar cell.

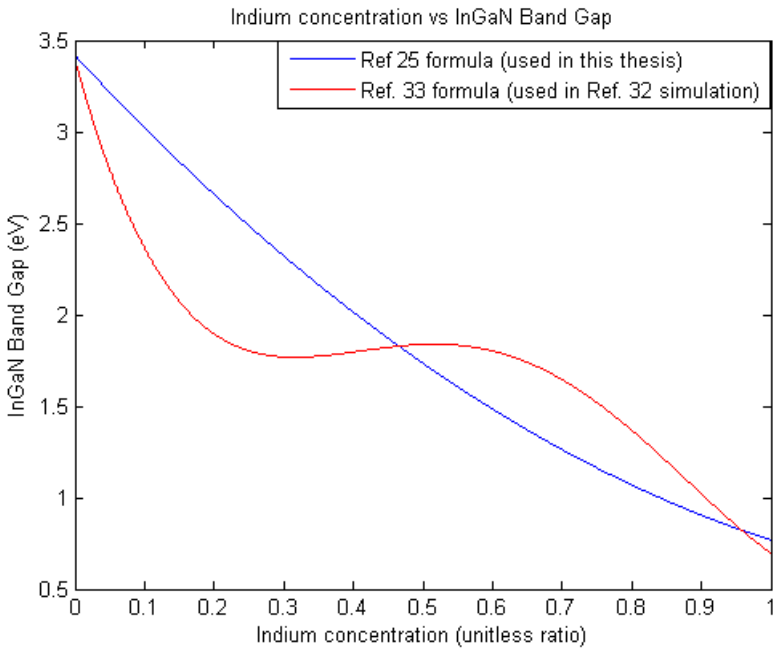

Figure 46. Comparison of InGaN band gap formulas

Number of junctions in the cell	I_{sc} (mA/cm^2)	V_{oc} (V)	Output peak power (mW/cm^2)	Efficiency (%)
2	27	1.22	26.48	27.485
3	18.2	2.22	32.42	33.642
4	13.5	3.28	35.48	36.825
5	11	4.28	37.68	39.105
6	9.1	5.34	38.88	40.346

Table 11. InGaN efficiency results (From [5]).

The differences in efficiency results can be partly attributed to the difference in band gap formula used. For example, $In_{0.20}Ga_{0.80}N$ has a band gap of 2.66 eV with the formula used in this thesis. The formula from [37] yields a band gap of 1.897 eV. If the $In_{0.20}Ga_{0.80}N$ band gap of 1.897 eV is substituted in the single-junction solar cell simulation of this thesis, the efficiency decreases significantly. Figure 47 compares the IV output for $In_{0.20}Ga_{0.80}N$ at Eg=1.897 eV and Eg=2.66 eV.

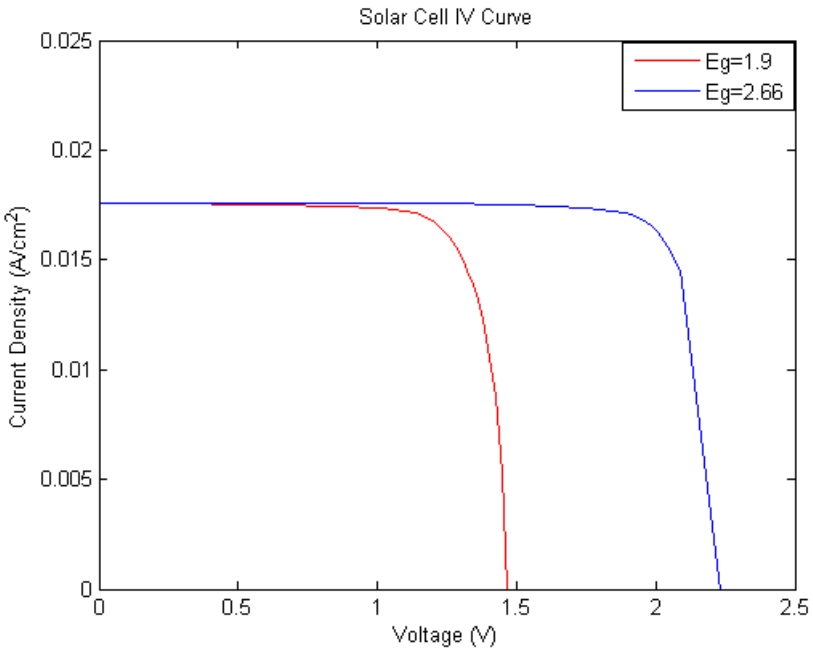

Figure 47. IV curve for $In_{0.20}Ga_{0.80}N$ using different band gaps

The efficiency of the $In_{0.20}Ga_{0.80}N$ (2.66 eV) single-junction solar cell simulated in this thesis was 24.32%. Changing the band gap to 1.897 eV yields an efficiency of 14.94%. This is a significant decrease. However, the band gap for the other three junctions increases with the formula used in [37]. The quad-junction simulation was run with the new band gaps. Figure 48 shows the IV curve for the quad-junction solar cell. The efficiency for the quad-junction solar cell increases to 43.62%. It is difficult to state which band gap model is more correct.

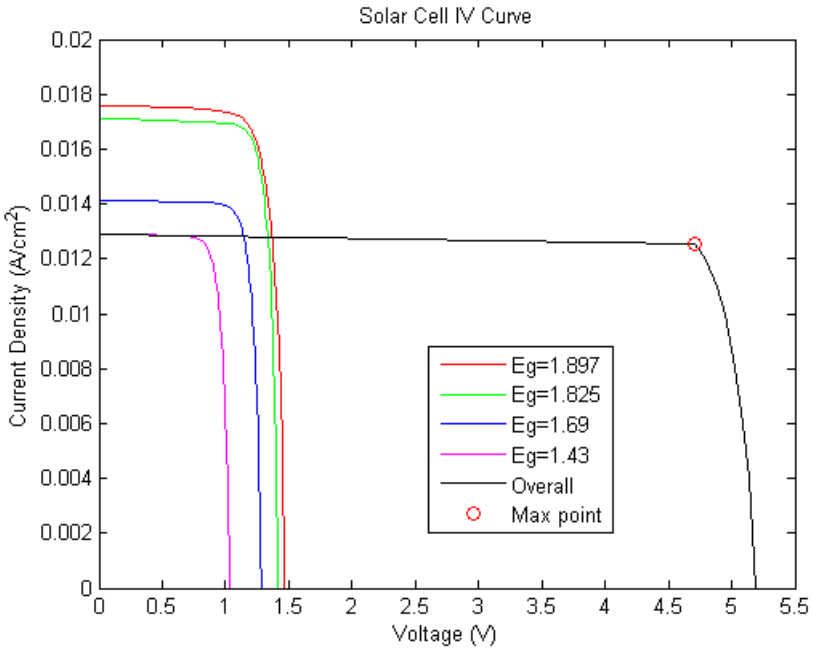

Figure 48. Quad-junction InGaN solar cell IV curve using calculated band gaps from [37] formula.

Material	Isc (mA/cm^2)	Voc (V)	Fill factor	Efficiency
$In_{0.20}Ga_{0.80}N$ $In_{0.57}Ga_{0.43}N$ $In_{0.68}Ga_{0.32}N$ $In_{0.78}Ga_{0.22}N$ Quad-junction	12.9	5.194	88.06%	43.62

Table 12. Quad junction InGaN efficiency using band gaps from [37] calculations.

A common finding in [5] and this thesis is that both simulations show that Indium Gallium Nitride multijunction solar cells can provide a significant improvement in solar cell efficiency. However, this is the first time that a Technology Computer Aided Design (TCAD), such as Silvaco Atlas, has been used to simulate InGaN solar cells.

The results of this thesis simulation demonstrate that Indium Gallium Nitride is potentially an excellent semiconductor photovoltaic material. The material science research in the future can confirm these outcomes in the future.

Production of single-junction solar cells appears to be the first step to be taken. Once the photovoltaic properties are demonstrated with actual Indium Gallium Nitride, the complexity of dual-junction solar cells can be addressed. Tunnel junctions made up of Indium Gallium Nitride may need to be explored as well.

THIS PAGE LEFT INTENTIONALLY BLANK

VI. CONCLUSIONS AND RECOMMENDATIONS

A. RESULTS AND CONCLUSIONS

Indium Gallium Nitride is a semiconductor material with potential to be used in photovoltaic devices. A new simulation was performed using Silvaco Atlas. The results of the quad-junction Indium Gallium Nitride solar cell indicate that a new high-efficiency material should be produced. Current state-of-the-art multijunction solar cells have efficiencies in the 30-33% range. The 41% efficiency predicted in this thesis is the highest of all simulations performed at the Naval Postgraduate School using Silvaco Atlas.

B. RECOMMENDATIONS FOR FUTURE RESEARCH

There are multiple areas that can be explored in future research. This thesis focused on the development of a solar cell model that emphasizes the use of optical constants (refraction and extinction coefficients n and k). The model used default settings for other parameters, such as permittivity, affinity, radiative recombination rate, electron and hole lifetimes, electron and hole density of states, and lattice constants. One area of future research is to obtain measured data for the above parameters. This subject is critical in improving the model. The other option is to interpolate from known values. Additionally, the inclusion of tunnel junctions in the simulation is of great value.

Other areas of research include finding different semiconductor materials that offer potential for high-efficiency solar cells. Lawrence Berkeley National Laboratory is also working with multiband materials, such as Zinc Manganese Tellerium Oxide (ZnMnTeO). This type of material offers a single junction solar cell, but there are multiple band gaps within the single junction.

One more recommended path is to optimize the physical parameters of the solar cell. The thickness of each of the layers can be optimized to produce a better efficiency. The band gap distribution for a quad-junction solar cell can be improved to obtain higher efficiency. It should be noted that obtaining the correct optical data for these band gaps is essential.

APPENDIX A: SILVACO ATLAS INPUT DECK

The code for the quad-junction InGaN solar cell was broken down into four single-junction solar cells. This was done because the material properties of InGaN had to be changed for each of the junctions.

Original code for the Silvaco Atlas input deck was obtained from Michalopolous [1], Bates, [2], Green [3], and Canfield [4]. Modifications to the code were made to support this thesis.

A. TOP JUNCTION: $IN_{0.20}GA_{0.80}N$, EG=2.66 EV

```
go atlas


set cellWidth=5.000000e+002
set capWidthpercent=8.000000e+000
set divs=1.000000e+001
set contThick=1.000000e-001
set capThick=3.000000e-001
set capDop=1.000000e+020
set windowThick=0.01
set winDop=2.15e17
set emitterThick=0.01
#changed emitDop from 1e16 to 1e20
set emitDop=1e16
set baseThick=3.19467
#changed basDop from 1e16 to 1e20
set baseDop=1e16
set bsfThick=0.03533
set bsfDop=2.15e19

set cellWidthDiv=$cellWidth/$divs
set width3d=100e6/$cellWidth
set capWidth=0.01*$capWidthpercent*$cellWidth/2
set capWidthDiv=$capWidth/($divs/2)
set cellWidthHalf=$cellWidth/2

set bsfLo=0
set bsfHi=$bsfLo-$bsfThick
set bsfDiv=$bsfThick/$divs

set baseLo=$bsfHi
set baseHi=$baseLo-$baseThick
set baseMid=$baseLo-$baseThick/2
set baseDiv=$baseThick/$divs

set emitterLo=$baseHi
```

```
set emitterHi=$emitterLo-$emitterThick
set emitterDiv=$emitterThick/$divs

set windowLo=$emitterHi
set windowHi=$windowLo-$windowThick
set windowDiv=$windowThick/$divs

set capLo=$windowHi
set capHi=$capLo-$capThick
#set capDiv=$capThick/$divs

set contLo=$capHi
set contHi=$contLo-$contThick
set contDiv=$contThick/$divs

set lightY=$emitterHi-5

mesh width=$width3d
## X-Mesh
x.mesh loc=-$cellWidthHalf spac=$cellWidthDiv
x.mesh loc=-$capWidth spac=$capWidthDiv
x.mesh loc=$capWidth spac=$capWidthDiv
x.mesh loc=$cellWidthHalf spac=$cellWidthDiv

## Y-Mesh
# Top contact
y.mesh loc=$contHi spac=0
y.mesh loc=$contLo spac=0
# Cap
# Window
y.mesh loc=$windowHi spac=$windowDiv
y.mesh loc=$windowLo spac=$windowDiv
# Emitter
y.mesh loc=$emitterLo spac=$emitterDiv
# Base
y.mesh loc=$baseMid spac=$baseDiv
# BSF
y.mesh loc=$bsfHi spac=$bsfDiv
y.mesh loc=$bsfLo spac=$bsfDiv


## Regions
# Cap
#region  num=8  material=Vacuum  x.min=-$capWidth  x.max=$capWidth  y.min=$contHi
y.max=$contLo
region  num=1  material=InGaN  x.min=-$capWidth  x.max=$capWidth  y.min=$capHi
y.max=$capLo x.comp=0.20
region    num=2    material=Vacuum    x.min=-$cellWidthHalf    x.max=-$capWidth
y.min=$contHi y.max=$capLo
region num=3 material=Vacuum x.min=$capWidth x.max=$cellWidthHalf y.min=$contHi
y.max=$capLo
# Window [for Ge cell, use AlGaAs with x.comp=0.2]
region   num=4   material=InGaN   x.min=-$cellWidthHalf   x.max=$cellWidthHalf
y.min=$windowHi y.max=$windowLo x.comp=0.20

#region     num=4     material=AlGaAs     x.comp=0.2     x.min=-$cellWidthHalf
x.max=$cellWidthHalf y.min=$windowHi y.max=$windowLo
# Emitter
region   num=5   material=InGaN   x.min=-$cellWidthHalf   x.max=$cellWidthHalf
y.min=$emitterHi y.max=$emitterLo x.comp=0.20
# Base
```

```
region    num=6    material=InGaN    x.min=-$cellWidthHalf    x.max=$cellWidthHalf
y.min=$baseHi y.max=$baseLo x.comp=0.20
# BSF
region    num=7    material=InGaN    x.min=-$cellWidthHalf    x.max=$cellWidthHalf
y.min=$bsfHi y.max=$bsfLo x.comp=0.20

##  Electrodes  [for  InGaP  cell,  add  cathode  (gold)  and  remove  cathode
(conductor)]
electrode    name=cathode    material=Gold    x.min=-$capWidth    x.max=$capWidth
y.min=$contHi y.max=$contLo
#electrode      name=cathode      x.min=-$cellWidthHalf      x.max=$cellWidthHalf
y.min=$windowHi y.max=$windowHi
electrode  name=anode  x.min=-$cellWidthHalf  x.max=$cellWidthHalf  y.min=$bsfLo
y.max=$bsfLo

## Doping [for InGaP cell, uncomment cap doping]
# Cap
doping uniform region=1 n.type conc=$capDop
# Window
doping uniform region=4 n.type conc=$winDop
# Emitter
doping uniform region=5 n.type conc=$emitDop
# Base
doping uniform region=6 p.type conc=$baseDop
# BSF
doping uniform region=7 p.type conc=$bsfDop

## Material properties
# Opaque contact [comment out for InGaP cell]
#material region=8 real.index=1.2 imag.index=1.8
# Vacuum (for zero reflection) [change to match window material (InGaP use
Vacuum_AlInP)]
#                              [for InGaP cell, comment out region 1]
#material region=1 index.file=Vacuum_InGaP.opt
material region=2 index.file=VacuumIn20Ga80N.opt
material region=3 index.file=VacuumIn20Ga80N.opt

#InGaN
material material=InGaN EG300=2.6612 index.file=In20Ga80N.opt

# Gold
material material=Gold real.index=1.2 imag.index=1.8


## Models [InGaP cell, 1; GaAs cell, 5&6; InGaNAs cell, 7]
models region=1 CONMOB
MODELS CHUANG CONMOB FLDMOB SRH OPTR PRINT

## Light beams [GaAs b1,0.55-0.75,200 b2,0.75-0.88,65] 0.12-2.7,50 [630,825]
beam     num=1     x.origin=0     y.origin=$lightY     angle=90     back.refl
power.file=AM0nrel.spec \
  wavel.start=0.12 wavel.end=2.4 wavel.num=50

struct outfile=SingleCell_webf.str
#tonyplot SingleCell_webf.str

solve init
method gummel newton maxtraps=10 itlimit=25
solve b1=0.9

## Getting Isc for I-V curve points
method newton maxtraps=10 itlimit=100
```

```
solve b1=0.95
extract name="isc" max(i."cathode")
set isc=$isc*$width3d
set i1=$isc/10
set i2=$i1+$isc/10
set i3=$i2+$isc/10
set i4=$i3+$isc/10
set i5=$i4+$isc/10
set i6=$i5+$isc/20
set i7=$i6+$isc/20
set i8=$i7+$isc/20
set i9=$i8+$isc/20
set i10=$i9+$isc/20
set i11=$i10+$isc/40
set i12=$i11+$isc/40
set i13=$i12+$isc/40
set i14=$i13+$isc/40
set i15=$i14+$isc/40
set i16=$i15+$isc/80
set i17=$i16+$isc/80
set i18=$i17+$isc/80
set i19=$i18+$isc/80
set i20=$i19+$isc/80
set i21=$i20+$isc/80
set i22=$i21+$isc/80
set i23=$i22+$isc/80
set i24=$i23+$isc/80
set i25=$i24+$isc/80-0.00001
##

log outfile=In20Ga80N.log

method newton maxtraps=10 itlimit=100
solve b1=0.95

contact name=anode current
method newton maxtraps=10 itlimit=100

## Pmax points [InGaP 18-25; GaAs 15-25; InGaNAs 13-25; Ge 11-25]
solve ianode=-$i25 b1=0.95
solve ianode=-$i24 b1=0.95
solve ianode=-$i23 b1=0.95
solve ianode=-$i22 b1=0.95
solve ianode=-$i21 b1=0.95
solve ianode=-$i20 b1=0.95
solve ianode=-$i19 b1=0.95
solve ianode=-$i18 b1=0.95
solve ianode=-$i17 b1=0.95
solve ianode=-$i16 b1=0.95
solve ianode=-$i15 b1=0.95
solve ianode=-$i14 b1=0.95
solve ianode=-$i13 b1=0.95
solve ianode=-$i12 b1=0.95
solve ianode=-$i11 b1=0.95
solve ianode=-$i10 b1=0.95
solve ianode=-$i9 b1=0.95
solve ianode=-$i8 b1=0.95
solve ianode=-$i7 b1=0.95
solve ianode=-$i6 b1=0.95
solve ianode=-$i5 b1=0.95
solve ianode=-$i4 b1=0.95
solve ianode=-$i3 b1=0.95
```

```
solve ianode=-$i2 b1=0.95
solve ianode=-$i1 b1=0.95

solve ianode=0 b1=0.95
log off
extract name="iv" curve(v."anode", i."cathode") outfile="IVcurveIn20Ga80N.dat"
tonyplot IVcurveIn20Ga80N.dat

log outfile=doneIn20Ga80N.log
log off
```

B. SECOND JUNCTION: $IN_{0.57}GA_{0.43}N$, EG=1.6 EV

```
go atlas

set cellWidth=5.000000e+002
set capWidthpercent=8.000000e+000
set divs=1.000000e+001
set contThick=1.000000e-001
set capThick=3.000000e-001
set capDop=1.000000e+020
set windowThick=0.01
set winDop=2.15e17
set emitterThick=0.01
#changed emitDop from 1e16 to 1e20
set emitDop=1e16
set baseThick=3.19467
#changed basDop from 1e16 to 1e20
set baseDop=1e16
set bsfThick=0.03533
set bsfDop=2.15e19

set cellWidthDiv=$cellWidth/$divs
set width3d=100e6/$cellWidth
set capWidth=0.01*$capWidthpercent*$cellWidth/2
set capWidthDiv=$capWidth/($divs/2)
set cellWidthHalf=$cellWidth/2

set bsfLo=0
set bsfHi=$bsfLo-$bsfThick
set bsfDiv=$bsfThick/$divs

set baseLo=$bsfHi
set baseHi=$baseLo-$baseThick
set baseMid=$baseLo-$baseThick/2
set baseDiv=$baseThick/$divs

set emitterLo=$baseHi
set emitterHi=$emitterLo-$emitterThick
set emitterDiv=$emitterThick/$divs

set windowLo=$emitterHi
set windowHi=$windowLo-$windowThick
set windowDiv=$windowThick/$divs

set capLo=$windowHi
set capHi=$capLo-$capThick
#set capDiv=$capThick/$divs

set contLo=$capHi
set contHi=$contLo-$contThick
```

```
set contDiv=$contThick/$divs

set lightY=$emitterHi-5

mesh width=$width3d
## X-Mesh
x.mesh loc=-$cellWidthHalf spac=$cellWidthDiv
x.mesh loc=-$capWidth spac=$capWidthDiv
x.mesh loc=$capWidth spac=$capWidthDiv
x.mesh loc=$cellWidthHalf spac=$cellWidthDiv

## Y-Mesh
# Top contact
y.mesh loc=$contHi spac=0
y.mesh loc=$contLo spac=0
# Cap
# Window
y.mesh loc=$windowHi spac=$windowDiv
y.mesh loc=$windowLo spac=$windowDiv
# Emitter
y.mesh loc=$emitterLo spac=$emitterDiv
# Base
y.mesh loc=$baseMid spac=$baseDiv
# BSF
y.mesh loc=$bsfHi spac=$bsfDiv
y.mesh loc=$bsfLo spac=$bsfDiv


## Regions
# Cap
#region num=8 material=Vacuum x.min=-$capWidth x.max=$capWidth y.min=$contHi
y.max=$contLo
region num=1 material=InGaN x.min=-$capWidth x.max=$capWidth y.min=$capHi
y.max=$capLo x.comp=0.57
region num=2 material=Vacuum x.min=-$cellWidthHalf x.max=-$capWidth
y.min=$contHi y.max=$capLo
region num=3 material=Vacuum x.min=$capWidth x.max=$cellWidthHalf y.min=$contHi
y.max=$capLo
# Window [for Ge cell, use AlGaAs with x.comp=0.2]
region num=4 material=InGaN x.min=-$cellWidthHalf x.max=$cellWidthHalf
y.min=$windowHi y.max=$windowLo x.comp=0.57

#region num=4 material=AlGaAs x.comp=0.2 x.min=-$cellWidthHalf
x.max=$cellWidthHalf y.min=$windowHi y.max=$windowLo
# Emitter
region num=5 material=InGaN x.min=-$cellWidthHalf x.max=$cellWidthHalf
y.min=$emitterHi y.max=$emitterLo x.comp=0.57
# Base
region num=6 material=InGaN x.min=-$cellWidthHalf x.max=$cellWidthHalf
y.min=$baseHi y.max=$baseLo x.comp=0.57
# BSF
region num=7 material=InGaN x.min=-$cellWidthHalf x.max=$cellWidthHalf
y.min=$bsfHi y.max=$bsfLo x.comp=0.57

## Electrodes [for InGaP cell, add cathode (gold) and remove cathode
(conductor)]
electrode name=cathode material=Gold x.min=-$capWidth x.max=$capWidth
y.min=$contHi y.max=$contLo
#electrode name=cathode x.min=-$cellWidthHalf x.max=$cellWidthHalf
y.min=$windowHi y.max=$windowHi
electrode name=anode x.min=-$cellWidthHalf x.max=$cellWidthHalf y.min=$bsfLo
y.max=$bsfLo
```

```
## Doping [for InGaP cell, uncomment cap doping]
# Cap
doping uniform region=1 n.type conc=$capDop
# Window
doping uniform region=4 n.type conc=$winDop
# Emitter
doping uniform region=5 n.type conc=$emitDop
# Base
doping uniform region=6 p.type conc=$baseDop
# BSF
doping uniform region=7 p.type conc=$bsfDop

## Material properties
# Opaque contact [comment out for InGaP cell]
#material region=8 real.index=1.2 imag.index=1.8
# Vacuum (for zero reflection) [change to match window material (InGaP use
Vacuum_AlInP)]
#                              [for InGaP cell, comment out region 1]
material region=2 index.file=VacuumIn57Ga43N.opt
material region=3 index.file=VacuumIn57Ga43N.opt
# GaAs

#InGaN
material material=InGaN EG300=1.559 index.file=In57Ga43N.opt

# Gold
material material=Gold real.index=1.2 imag.index=1.8



## Models [InGaP cell, 1; GaAs cell, 5&6; InGaNAs cell, 7]
models region=1 CONMOB
MODELS CHUANG CONMOB FLDMOB SRH OPTR PRINT

## Light beams [GaAs b1,0.55-0.75,200 b2,0.75-0.88,65] 0.12-2.7,50 [630,825]
beam      num=1      x.origin=0      y.origin=$lightY      angle=90      back.refl
power.file=PostJunction1.spec.txt \
  wavel.start=0.12 wavel.end=2.4 wavel.num=50

struct outfile=SingleCell_webf.str
#tonyplot SingleCell_webf.str

solve init
method gummel newton maxtraps=10 itlimit=25
solve b1=0.9

## Getting Isc for I-V curve points
method newton maxtraps=10 itlimit=100
solve b1=0.95
extract name="isc" max(i."cathode")
set isc=$isc*$width3d
set i1=$isc/10
set i2=$i1+$isc/10
set i3=$i2+$isc/10
set i4=$i3+$isc/10
set i5=$i4+$isc/10
set i6=$i5+$isc/20
set i7=$i6+$isc/20
set i8=$i7+$isc/20
set i9=$i8+$isc/20
set i10=$i9+$isc/20
```

```
set i11=$i10+$isc/40
set i12=$i11+$isc/40
set i13=$i12+$isc/40
set i14=$i13+$isc/40
set i15=$i14+$isc/40
set i16=$i15+$isc/80
set i17=$i16+$isc/80
set i18=$i17+$isc/80
set i19=$i18+$isc/80
set i20=$i19+$isc/80
set i21=$i20+$isc/80
set i22=$i21+$isc/80
set i23=$i22+$isc/80
set i24=$i23+$isc/80
set i25=$i24+$isc/80-0.00001
##

log outfile=In57Ga43N.log

method newton maxtraps=10 itlimit=100
solve b1=0.95

contact name=anode current
method newton maxtraps=10 itlimit=100

## Pmax points [InGaP 18-25; GaAs 15-25; InGaNAs 13-25; Ge 11-25]
solve ianode=-$i25 b1=0.95
solve ianode=-$i24 b1=0.95
solve ianode=-$i23 b1=0.95
solve ianode=-$i22 b1=0.95
solve ianode=-$i21 b1=0.95
solve ianode=-$i20 b1=0.95
solve ianode=-$i19 b1=0.95
solve ianode=-$i18 b1=0.95
solve ianode=-$i17 b1=0.95
solve ianode=-$i16 b1=0.95
solve ianode=-$i15 b1=0.95
solve ianode=-$i14 b1=0.95
solve ianode=-$i13 b1=0.95
solve ianode=-$i12 b1=0.95
solve ianode=-$i11 b1=0.95
solve ianode=-$i10 b1=0.95
solve ianode=-$i9 b1=0.95
solve ianode=-$i8 b1=0.95
solve ianode=-$i7 b1=0.95
solve ianode=-$i6 b1=0.95
solve ianode=-$i5 b1=0.95
solve ianode=-$i4 b1=0.95
solve ianode=-$i3 b1=0.95
solve ianode=-$i2 b1=0.95
solve ianode=-$i1 b1=0.95
##

solve ianode=0 b1=0.95

log off
extract name="iv" curve(v."anode", i."cathode") outfile="IVcurveIn57Ga43N.dat"
tonyplot IVcurveIn57Ga43N.dat

log outfile=doneIn57Ga43N.log
log off
```

C. THIRD JUNCTION: $IN_{0.68}GA_{0.32}N$, EG=1.31 EV

```
go atlas


set cellWidth=5.000000e+002
set capWidthpercent=8.000000e+000
set divs=1.000000e+001
set contThick=1.000000e-001
set capThick=3.000000e-001
set capDop=1.000000e+020
set windowThick=0.01
set winDop=2.15e17
set emitterThick=0.01
#changed emitDop from 1e16 to 1e20
set emitDop=1e16
set baseThick=3.19467
#changed basDop from 1e16 to 1e20
set baseDop=1e16
set bsfThick=0.03533
set bsfDop=2.15e19

set cellWidthDiv=$cellWidth/$divs
set width3d=100e6/$cellWidth
set capWidth=0.01*$capWidthpercent*$cellWidth/2
set capWidthDiv=$capWidth/($divs/2)
set cellWidthHalf=$cellWidth/2

set bsfLo=0
set bsfHi=$bsfLo-$bsfThick
set bsfDiv=$bsfThick/$divs

set baseLo=$bsfHi
set baseHi=$baseLo-$baseThick
set baseMid=$baseLo-$baseThick/2
set baseDiv=$baseThick/$divs

set emitterLo=$baseHi
set emitterHi=$emitterLo-$emitterThick
set emitterDiv=$emitterThick/$divs

set windowLo=$emitterHi
set windowHi=$windowLo-$windowThick
set windowDiv=$windowThick/$divs

set capLo=$windowHi
set capHi=$capLo-$capThick
#set capDiv=$capThick/$divs

set contLo=$capHi
set contHi=$contLo-$contThick
set contDiv=$contThick/$divs

set lightY=$emitterHi-5

mesh width=$width3d
## X-Mesh
x.mesh loc=-$cellWidthHalf spac=$cellWidthDiv
x.mesh loc=-$capWidth spac=$capWidthDiv
x.mesh loc=$capWidth spac=$capWidthDiv
x.mesh loc=$cellWidthHalf spac=$cellWidthDiv
```

```
## Y-Mesh
# Top contact
y.mesh loc=$contHi spac=0
y.mesh loc=$contLo spac=0
# Cap
# Window
y.mesh loc=$windowHi spac=$windowDiv
y.mesh loc=$windowLo spac=$windowDiv
# Emitter
y.mesh loc=$emitterLo spac=$emitterDiv
# Base
y.mesh loc=$baseMid spac=$baseDiv
# BSF
y.mesh loc=$bsfHi spac=$bsfDiv
y.mesh loc=$bsfLo spac=$bsfDiv


## Regions
# Cap
#region num=8 material=Vacuum x.min=-$capWidth x.max=$capWidth y.min=$contHi
y.max=$contLo
region num=1 material=InGaN x.min=-$capWidth x.max=$capWidth y.min=$capHi
y.max=$capLo x.comp=0.68
region num=2 material=Vacuum x.min=-$cellWidthHalf x.max=-$capWidth
y.min=$contHi y.max=$capLo
region num=3 material=Vacuum x.min=$capWidth x.max=$cellWidthHalf y.min=$contHi
y.max=$capLo
# Window [for Ge cell, use AlGaAs with x.comp=0.2]
region num=4 material=InGaN x.min=-$cellWidthHalf x.max=$cellWidthHalf
y.min=$windowHi y.max=$windowLo x.comp=0.68

#region num=4 material=AlGaAs x.comp=0.2 x.min=-$cellWidthHalf
x.max=$cellWidthHalf y.min=$windowHi y.max=$windowLo
# Emitter
region num=5 material=InGaN x.min=-$cellWidthHalf x.max=$cellWidthHalf
y.min=$emitterHi y.max=$emitterLo x.comp=0.68
# Base
region num=6 material=InGaN x.min=-$cellWidthHalf x.max=$cellWidthHalf
y.min=$baseHi y.max=$baseLo x.comp=0.68
# BSF
region num=7 material=InGaN x.min=-$cellWidthHalf x.max=$cellWidthHalf
y.min=$bsfHi y.max=$bsfLo x.comp=0.68

## Electrodes [for InGaP cell, add cathode (gold) and remove cathode
(conductor)]
electrode name=cathode material=Gold x.min=-$capWidth x.max=$capWidth
y.min=$contHi y.max=$contLo
#electrode name=cathode x.min=-$cellWidthHalf x.max=$cellWidthHalf
y.min=$windowHi y.max=$windowHi
electrode name=anode x.min=-$cellWidthHalf x.max=$cellWidthHalf y.min=$bsfLo
y.max=$bsfLo

## Doping [for InGaP cell, uncomment cap doping]
# Cap
doping uniform region=1 n.type conc=$capDop
# Window
doping uniform region=4 n.type conc=$winDop
# Emitter
doping uniform region=5 n.type conc=$emitDop
# Base
doping uniform region=6 p.type conc=$baseDop
```

```
# BSF
doping uniform region=7 p.type conc=$bsfDop

## Material properties
# Opaque contact [comment out for InGaP cell]
#material region=8 real.index=1.2 imag.index=1.8
# Vacuum (for zero reflection)
material region=2 index.file=VacuumIn68Ga32N.opt
material region=3 index.file=VacuumIn68Ga32N.opt

#InGaN
material material=InGaN EG300=1.3068 index.file=In68Ga32N.opt

# Gold
material material=Gold real.index=1.2 imag.index=1.8


## Models [InGaP cell, 1; GaAs cell, 5&6; InGaNAs cell, 7]
models region=1 CONMOB
MODELS CONMOB FLDMOB SRH OPTR PRINT

## Light beams [GaAs b1,0.55-0.75,200 b2,0.75-0.88,65] 0.12-2.7,50 [630,825]
beam      num=1      x.origin=0      y.origin=$lightY      angle=90      back.refl
power.file=PostJunction2.spec.txt \
  wavel.start=0.12 wavel.end=2.4 wavel.num=50

struct outfile=SingleCell_webf.str
#tonyplot SingleCell_webf.str

solve init
method gummel newton maxtraps=10 itlimit=25
solve b1=0.9

## Getting Isc for I-V curve points
method newton maxtraps=10 itlimit=100
solve b1=0.95
extract name="isc" max(i."cathode")
set isc=$isc*$width3d
set i1=$isc/10
set i2=$i1+$isc/10
set i3=$i2+$isc/10
set i4=$i3+$isc/10
set i5=$i4+$isc/10
set i6=$i5+$isc/20
set i7=$i6+$isc/20
set i8=$i7+$isc/20
set i9=$i8+$isc/20
set i10=$i9+$isc/20
set i11=$i10+$isc/40
set i12=$i11+$isc/40
set i13=$i12+$isc/40
set i14=$i13+$isc/40
set i15=$i14+$isc/40
set i16=$i15+$isc/80
set i17=$i16+$isc/80
set i18=$i17+$isc/80
set i19=$i18+$isc/80
set i20=$i19+$isc/80
set i21=$i20+$isc/80
set i22=$i21+$isc/80
set i23=$i22+$isc/80
set i24=$i23+$isc/80
```

```
set i25=$i24+$isc/80-0.00001
##

log outfile=In68Ga32N.log

method newton maxtraps=10 itlimit=100
solve b1=0.95

contact name=anode current
method newton maxtraps=10 itlimit=100

## Pmax points [InGaP 18-25; GaAs 15-25; InGaNAs 13-25; Ge 11-25]
solve ianode=-$i25 b1=0.95
solve ianode=-$i24 b1=0.95
solve ianode=-$i23 b1=0.95
solve ianode=-$i22 b1=0.95
solve ianode=-$i21 b1=0.95
solve ianode=-$i20 b1=0.95
solve ianode=-$i19 b1=0.95
solve ianode=-$i18 b1=0.95
solve ianode=-$i17 b1=0.95
solve ianode=-$i16 b1=0.95
solve ianode=-$i15 b1=0.95
solve ianode=-$i14 b1=0.95
solve ianode=-$i13 b1=0.95
solve ianode=-$i12 b1=0.95
solve ianode=-$i11 b1=0.95
solve ianode=-$i10 b1=0.95
solve ianode=-$i9 b1=0.95
solve ianode=-$i8 b1=0.95
solve ianode=-$i7 b1=0.95
solve ianode=-$i6 b1=0.95
solve ianode=-$i5 b1=0.95
solve ianode=-$i4 b1=0.95
solve ianode=-$i3 b1=0.95
solve ianode=-$i2 b1=0.95
solve ianode=-$i1 b1=0.95
##

solve ianode=0 b1=0.95

log off
extract name="iv" curve(v."anode", i."cathode") outfile="IVcurveIn68Ga32N.dat"
tonyplot IVcurveIn68Ga32N.dat

log outfile=doneIn68Ga32N.log
log off
```

D. BOTTOM JUNCTION: $IN_{0.78}GA_{0.22}N$, EG=1.11 EV

```
go atlas


set cellWidth=5.000000e+002
set capWidthpercent=8.000000e+000
set divs=1.000000e+001
set contThick=1.000000e-001
set capThick=3.000000e-001
set capDop=1.000000e+020
```

```
set windowThick=0.01
set winDop=2.15e17
set emitterThick=0.01
#changed emitDop from 1e16 to 1e20
set emitDop=1e16
set baseThick=3.19467
#changed basDop from 1e16 to 1e20
set baseDop=1e16
set bsfThick=0.03533
set bsfDop=2.15e19

set cellWidthDiv=$cellWidth/$divs
set width3d=100e6/$cellWidth
set capWidth=0.01*$capWidthpercent*$cellWidth/2
set capWidthDiv=$capWidth/($divs/2)
set cellWidthHalf=$cellWidth/2

set bsfLo=0
set bsfHi=$bsfLo-$bsfThick
set bsfDiv=$bsfThick/$divs

set baseLo=$bsfHi
set baseHi=$baseLo-$baseThick
set baseMid=$baseLo-$baseThick/2
set baseDiv=$baseThick/$divs

set emitterLo=$baseHi
set emitterHi=$emitterLo-$emitterThick
set emitterDiv=$emitterThick/$divs

set windowLo=$emitterHi
set windowHi=$windowLo-$windowThick
set windowDiv=$windowThick/$divs

set capLo=$windowHi
set capHi=$capLo-$capThick
#set capDiv=$capThick/$divs

set contLo=$capHi
set contHi=$contLo-$contThick
set contDiv=$contThick/$divs

set lightY=$emitterHi-5

mesh width=$width3d
## X-Mesh
x.mesh loc=-$cellWidthHalf spac=$cellWidthDiv
x.mesh loc=-$capWidth spac=$capWidthDiv
x.mesh loc=$capWidth spac=$capWidthDiv
x.mesh loc=$cellWidthHalf spac=$cellWidthDiv

## Y-Mesh
# Top contact
y.mesh loc=$contHi spac=0
y.mesh loc=$contLo spac=0
# Cap
# Window
y.mesh loc=$windowHi spac=$windowDiv
y.mesh loc=$windowLo spac=$windowDiv
# Emitter
y.mesh loc=$emitterLo spac=$emitterDiv
# Base
```

```
y.mesh loc=$baseMid spac=$baseDiv
# BSF
y.mesh loc=$bsfHi spac=$bsfDiv
y.mesh loc=$bsfLo spac=$bsfDiv

## Regions
# Cap
#region num=8 material=Vacuum x.min=-$capWidth x.max=$capWidth y.min=$contHi
y.max=$contLo
region num=1 material=InGaN x.min=-$capWidth x.max=$capWidth y.min=$capHi
y.max=$capLo x.comp=0.78
region num=2 material=Vacuum x.min=-$cellWidthHalf x.max=-$capWidth
y.min=$contHi y.max=$capLo
region num=3 material=Vacuum x.min=$capWidth x.max=$cellWidthHalf y.min=$contHi
y.max=$capLo
# Window [for Ge cell, use AlGaAs with x.comp=0.2]
region num=4 material=InGaN x.min=-$cellWidthHalf x.max=$cellWidthHalf
y.min=$windowHi y.max=$windowLo x.comp=0.78

#region num=4 material=AlGaAs x.comp=0.2 x.min=-$cellWidthHalf
x.max=$cellWidthHalf y.min=$windowHi y.max=$windowLo
# Emitter
region num=5 material=InGaN x.min=-$cellWidthHalf x.max=$cellWidthHalf
y.min=$emitterHi y.max=$emitterLo x.comp=0.78
# Base
region num=6 material=InGaN x.min=-$cellWidthHalf x.max=$cellWidthHalf
y.min=$baseHi y.max=$baseLo x.comp=0.78
# BSF
region num=7 material=InGaN x.min=-$cellWidthHalf x.max=$cellWidthHalf
y.min=$bsfHi y.max=$bsfLo x.comp=0.78

## Electrodes [for InGaP cell, add cathode (gold) and remove cathode
(conductor)]
electrode name=cathode material=Gold x.min=-$capWidth x.max=$capWidth
y.min=$contHi y.max=$contLo
#electrode name=cathode x.min=-$cellWidthHalf x.max=$cellWidthHalf
y.min=$windowHi y.max=$windowHi
electrode name=anode x.min=-$cellWidthHalf x.max=$cellWidthHalf y.min=$bsfLo
y.max=$bsfLo

## Doping [for InGaP cell, uncomment cap doping]
# Cap
doping uniform region=1 n.type conc=$capDop
# Window
doping uniform region=4 n.type conc=$winDop
# Emitter
doping uniform region=5 n.type conc=$emitDop
# Base
doping uniform region=6 p.type conc=$baseDop
# BSF
doping uniform region=7 p.type conc=$bsfDop

## Material properties
# Opaque contact [comment out for InGaP cell]
#material region=8 real.index=1.2 imag.index=1.8
# Vacuum (for zero reflection)
material region=2 index.file=VacuumInGa22N.opt
material region=3 index.file=VacuumInGa22N.opt

#InGaN
material material=InGaN EG300=1.1076 index.file=InGa22N.opt
```

```
# Gold
material material=Gold real.index=1.2 imag.index=1.8



## Models [InGaP cell, 1; GaAs cell, 5&6; InGaNAs cell, 7]
models region=1 CONMOB
MODELS CONMOB FLDMOB SRH OPTR PRINT

## Light beams [GaAs b1,0.55-0.75,200 b2,0.75-0.88,65] 0.12-2.7,50 [630,825]
beam      num=1      x.origin=0      y.origin=$lightY      angle=90      back.refl
power.file=PostJunction3.spec.txt \
  wavel.start=0.12 wavel.end=2.4 wavel.num=50

struct outfile=SingleCell_webf.str
#tonyplot SingleCell_webf.str

solve init
method gummel newton maxtraps=10 itlimit=25
solve b1=0.9

## Getting Isc for I-V curve points
method newton maxtraps=10 itlimit=100
solve b1=0.95
extract name="isc" max(i."cathode")
set isc=$isc*$width3d
set i1=$isc/10
set i2=$i1+$isc/10
set i3=$i2+$isc/10
set i4=$i3+$isc/10
set i5=$i4+$isc/10
set i6=$i5+$isc/20
set i7=$i6+$isc/20
set i8=$i7+$isc/20
set i9=$i8+$isc/20
set i10=$i9+$isc/20
set i11=$i10+$isc/40
set i12=$i11+$isc/40
set i13=$i12+$isc/40
set i14=$i13+$isc/40
set i15=$i14+$isc/40
set i16=$i15+$isc/80
set i17=$i16+$isc/80
set i18=$i17+$isc/80
set i19=$i18+$isc/80
set i20=$i19+$isc/80
set i21=$i20+$isc/80
set i22=$i21+$isc/80
set i23=$i22+$isc/80
set i24=$i23+$isc/80
set i25=$i24+$isc/80-0.00001
##

log outfile=In78Ga22N.log

method newton maxtraps=10 itlimit=100
solve b1=0.95

contact name=anode current
method newton maxtraps=10 itlimit=100

## Pmax points [InGaP 18-25; GaAs 15-25; InGaNAs 13-25; Ge 11-25]
```

```
solve ianode=-$i25 b1=0.95
solve ianode=-$i24 b1=0.95
solve ianode=-$i23 b1=0.95
solve ianode=-$i22 b1=0.95
solve ianode=-$i21 b1=0.95
solve ianode=-$i20 b1=0.95
solve ianode=-$i19 b1=0.95
solve ianode=-$i18 b1=0.95
solve ianode=-$i17 b1=0.95
solve ianode=-$i16 b1=0.95
solve ianode=-$i15 b1=0.95
solve ianode=-$i14 b1=0.95
solve ianode=-$i13 b1=0.95
solve ianode=-$i12 b1=0.95
solve ianode=-$i11 b1=0.95
solve ianode=-$i10 b1=0.95
solve ianode=-$i9 b1=0.95
solve ianode=-$i8 b1=0.95
solve ianode=-$i7 b1=0.95
solve ianode=-$i6 b1=0.95
solve ianode=-$i5 b1=0.95
solve ianode=-$i4 b1=0.95
solve ianode=-$i3 b1=0.95
solve ianode=-$i2 b1=0.95
solve ianode=-$i1 b1=0.95
##

solve ianode=0 b1=0.95

log off
extract name="iv" curve(v."anode", i."cathode") outfile="IVcurveIn78Ga22N.dat"
tonyplot IVcurveIn78Ga22N.dat

log outfile=doneIn78Ga22N.log

       log off
```

APPENDIX B: MATLAB CODE

The Matlab code provided in this appendix provided auxiliary support in the interpretation and display Sivaco Atlas log files.

Original code for some of the Matlab functions and scripts was obtained from Michalopolous [1], Bates, [2], Green [3], and Canfield [4]. Modifications to the code were made to support this thesis.

A. INDIUM GALLIUM NITRIDE BAND GAP CALCULATIONS

```
%InGaN Bandgap calculations
%Baldomero Garcia
clc;

%Constants

EgGaN=3.42;
EgInN=0.77;
b=1.43;
x=[0:0.0001:1];
% x=.67;
% InConcentration=x
% GaConcentration=1-x

%Formula for finding EgInGaN
EgInGaN=((1-x).*EgGaN)+(x.*EgInN)-(b.*x.*(1-x))

%Formula for finding x
solve('(((1-x)*EgGaN)+(x*EgInN)-(b*x*(1-x)))-EgInGaN','x');

% The other EgInGaN that we're solving for is EgInGaN=1.1
% EgInGaN=2.095
% Gacomp=1-(1/2/b*(EgGaN-EgInN+b-(EgGaN^2-2*EgInN*EgGaN-
2*b*EgGaN+EgInN^2-2*EgInN*b+b^2+4*b*EgInGaN)^(1/2)))
% Incomp=(1/2/b*(EgGaN-EgInN+b-(EgGaN^2-2*EgInN*EgGaN-
2*b*EgGaN+EgInN^2-2*EgInN*b+b^2+4*b*EgInGaN)^(1/2)))

%Plot
plot(x,EgInGaN,'b');
xlabel('Indium concentration (unitless ratio)');
ylabel('InGaN Band Gap (eV)');
title('Indium concentration vs InGaN Band Gap');
```

B. CONVERSION FROM DIELECTRIC CONSTANTS (EPSILONS) TO REFRACTION COEFFICIENTS (N, K)

Optical data needed to be provided n-k format. Some of the data obtained was available in epsilon form. Therefore, a conversion needed to be made. Michalopoulos generated the function below [1].

```
%   E2NK   Convert the e1, e2 pairs into n, k pairs.
% [n k] = E2NK(e1, e2)

% (c)2001 by P. Michalopoulos

function [n,k] = e2nk(e1, e2)

ap = (e1 + sqrt(e1.^2 + e2.^2)) / 2;
an = (e1 - sqrt(e1.^2 + e2.^2)) / 2;

app = ap >= 0;
anp = an >= 0;
err = (app < 0) & (anp < 0);
err = sum(err);
if err ~= 0
    disp('ERROR!')
end

a = ap .* app + an .* anp;

n = sqrt(a);

k = e2 ./ (2 * n);
```

C. CONVERSION FROM PHOTON ENERGY (EV) TO WAVELENGTH (UM)

Data was found in photon energy and wavelength form. In order to make comparisons, conversion from one form to another was necessary. Functions by Michalopoulos [1] are given below.

```
%   EV2UM   Converts photon energy (eV) into wavelength (um).

% (c)2001 by P. Michalopoulos

function um = ev2um(ev)
```

```
h = 6.6260755e-34;
eV = 1.60218e-19;
c = 2.99792458e8;

ev = ev * eV;
f = ev / h;
wavel = c ./ f;
um = wavel / 1e-6;


%   UM2EV   Converts photon wavelength (um) into energy (eV).

% (c)2001 by P. Michalopoulos

function ev = um2ev(um)

h = 6.6260755e-34;
eV = 1.60218e-19;
c = 2.99792458e8;

wavel = um * 1e-6;
f = c ./ wavel;
ev = h * f;
ev = ev ./ eV;
```

D. IV CURVE PLOTS FOR INDIUM GALLIUM NITRIDE QUAD JUNCTION SOLAR CELL

```
% Code modified from Canfield's source code
% Data obtained from log files from InGaN quad-junction solar cell
% Baldomero Garcia
clc;
% In20Ga80N with AM0 spectrum
current1=[0.0176131398  0.0176031407    0.0175505986    0.0174980573
0.0173929742    0.0171728094    0.0169526469    0.0167324843
0.0165123158    0.0162921532    0.0160719881    0.0158518253
0.0156316602    0.0154114983    0.0149711686    0.0145308402
0.0140905121    0.0136501825    0.0132098541    0.0123291993
0.0114485415    0.0105678837    0.0096872266    0.0088065691
0.0070452558    0.0052839419    0.0035226276    0.0017613142    -
0.0000000001];
voltage1=[0.0000000000  0.2970913579    1.1822462140    1.5075176680
1.7472436590    1.8900757790    1.9378145180    1.9663764170
1.9875670060    2.0047710060    2.0194136280    2.0322369610
2.0436835120    2.0540360290    2.0722008890    2.0877645130
2.1013319790    2.1132957310    2.1239292560    2.1419700890
2.1566166780    2.1686629450    2.1786938920    2.1871519430
2.2006132650    2.2108811030    2.2190289820    2.2257052930
2.2313181110];

% In57Ga43N with postjunction1 spectrum
```

```
current2=[0.0171128720  0.0171028783    0.0168989671    0.0166850573
0.0164711457    0.0162572338    0.0160433258    0.0158294126
0.0156155026    0.0154015923    0.0151876797    0.0149737698
0.0145459485    0.0141181240    0.0136903032    0.0132624807
0.0128346588    0.0119790166    0.0111233713    0.0102677280
0.0094120828    0.0085564398    0.0068451513    0.0051338641
0.0034225761    0.0017112879    -0.0000000001];
voltage2=[0.0000000000  0.1305081858    0.8192581792    0.9015131674
0.9331338594    0.9534997163    0.9689573887    0.9815965012
0.9923675261    1.0017892410    1.0101786220    1.0177449700
1.0309568480    1.0422028240    1.0519502020    1.0605082500
1.0680958050    1.0809744750    1.0915085520    1.1002972060
1.1077533400    1.1141715070    1.1247003520    1.1330384420
1.1398643710    1.1456000250    1.1505207070];

% In68Ga32N with postjunction2 spectrum
current3=[0.0141231105  0.0141131184    0.0140298496    0.0139465807
0.0137700408    0.0135935022    0.0134169620    0.0132404230
0.0130638854    0.0128873465    0.0127108077    0.0125342689
0.0123577303    0.0120046521    0.0116515739    0.0112984952
0.0109454185    0.0105923395    0.0098861822    0.0091800273
0.0084738721    0.0077677158    0.0070615601    0.0056492474
0.0042369367    0.0028246240    0.0014123119    0.0000000001];
voltage3=[0.0000000000  0.1311096030    0.5441673681    0.6320277025
0.6842499725    0.7083967768    0.7248954021    0.7377135412
0.7483143199    0.7574074704    0.7653951663    0.7725296065
0.7789805527    0.7902824668    0.7999460470    0.8083630634
0.8157932979    0.8224203640    0.8337763994    0.8431914560
0.8511524069    0.8579918718    0.8639469242    0.8738573284
0.8818299562    0.8884345077    0.8940340114    0.8988707325];

% In78Ga22N with potjunction3 spectrum
current4=[0.0128841840  0.0128741794    0.0127231275    0.0125620760
0.0124010228    0.0122399704    0.0120789198    0.0119178658
0.0117568129    0.0115957622    0.0114347108    0.0112736577
0.0109515531    0.0106294488    0.0103073439    0.0099852400
0.0096631342    0.0090189240    0.0083747191    0.0077305090
0.0070862990    0.0064420895    0.0051536706    0.0038652545
0.0025768364    0.0012884183    -0.0000000001];
voltage4=[0.0000000000  0.1078032006    0.4688474643    0.5100668879
0.5309258388    0.5454971566    0.5569116230    0.5663876299
0.5745324881    0.5816962863    0.5881009992    0.5938970077
0.6040640671    0.6127739225    0.6203776540    0.6271079482
0.6331288820    0.6434973415    0.6521554853    0.6595301586
0.6659109540    0.6715037308    0.6808929507    0.6885228391
0.6948948317    0.7003322584    0.7050534598];

% Combined
current5=[0 0.001991    0.004011    0.006003    0.007994    0.01001
0.01178 0.01198 0.0126  0.01275 0.01286 0.0128841840];
voltage5=[4.9793    4.9542  4.9195  4.8744  4.8185  4.7271  4.5995
4.5723  4.4736  4.3906  4.0906 0];

P1=current1.*voltage1;
[a b]=max(P1);
```

```
Pmax1=voltage1(b)*current1(b);
Voc1=max(voltage1);
Isc1=max(current1);
FF1=Pmax1/(Voc1*Isc1)
Eff1=100*Pmax1/(.1353)

P2=current2.*voltage2;
[c d]=max(P2);
Pmax2=voltage2(d)*current2(d);
Voc2=max(voltage2);
Isc2=max(current2);
FF2=Pmax2/(Voc2*Isc2)
Eff2=100*Pmax2/(.1353)

P3=current3.*voltage3;
[e f]=max(P3);
Pmax3=voltage3(f)*current3(f);
Voc3=max(voltage3);
Isc3=max(current3);
FF3=Pmax3/(Voc3*Isc3)
Eff3=100*Pmax3/(.1353)

P4=current4.*voltage4;
[g h]=max(P4);
Pmax4=voltage4(h)*current4(h);
Voc4=max(voltage4);
Isc4=max(current4);
FF4=Pmax4/(Voc4*Isc4)
Eff4=100*Pmax4/(.1353)

P5=current5.*voltage5;
[k l]=max(P5);
Pmax5=voltage5(l)*current5(l);
Voc5=max(voltage5);
Isc5=max(current5);
FF5=Pmax5/(Voc5*Isc5)
Eff5=100*Pmax5/(.1353)

plot(voltage1,current1,'r');
%grid on;
hold on;
%plot(voltage1(b),current1(b),'o');
hold on;
plot(voltage2,current2,'r');
hold on;
%plot(voltage2(d),current2(d),'o');
hold on;
plot(voltage3,current3,'r');
hold on;
%plot(voltage3(f),current3(f),'o');
hold on;
plot(voltage4,current4,'r');
hold on;
%plot(voltage4(h),current4(h),'o');
hold on;
```

```
plot(voltage5,current5,'b');
hold on;
plot(voltage5(l),current5(l),'or');
hold off;
xlabel('Voltage (V)')
ylabel('Current Density (A/cm^2)')
title('Solar Cell IV Curve')
axis([0 5.5 0 0.020])
```

E. AIR MASS ZERO PLOTS

Air Mass Zero (AM0) data was obtained from NREL [19] and plotted using the Matlab function provided by Michalopoulos [1]. It was modified to provide an additional plot.

```
%    AMSPECTRUMS   Plot the data contained in spectrums.mat
% Check the source code and uncomment the required lines.
% (c)2001 by P. Michalopoulos
h = 6.6260755e-34;
eV = 1.60218e-19;
c = 2.99792458e8;
load('Data\spectrums')
plot(AM0_wavel, AM0_int1, 'b', AM15a_wavel, AM15a_int1, 'r'), grid on
title('AM 0 and AM 1.5 spectra'), xlabel('Wavelength [um]'),
ylabel('Irradiance [W / cm^2*um]')
axis([0 3 0 0.23])
```

The code above was modified to display AM0 with respect to photon energy and wavelength, respectively.

```
Figure (1)
plot(um,iradiance,'r');
xlabel('Wavelength (um)')
ylabel('Irradiance W/cm^2*um')
title('AM0')
axis([0 2.5 0 0.25])
Figure (2)
plot(ev,iradiance,'b');
xlabel('Energy (eV)')
ylabel('Irradiance W/cm^2um')
title('AM0')
axis([0 6.0 0 0.25])
```

LIST OF REFERENCES

[1] P. Michalopoulous, “A novel approach for the development and optimization of state-of-the-art photovoltaic devices using Silvaco”, Master’s Thesis, Naval Postgraduate School, Monterey, California, 2002.

[2] A. D. Bates, “Novel optimization techniques for multijunction solar cell design using Silvaco Atlas”, Master’s Thesis, Naval Postgraduate School, Monterey, California, 2004.

[3] M. Green, “The verification of Silvaco as a solar cell simulation tool and the design and optimization of a four-junction solar cell”, Master’s Thesis, Naval Postgraduate School, Monterey, California, 2003.

[4] B. J. Canfield, “Advanced modeling of high temperature performance of Indium Gallium Arsenide thermophotovoltaic cells”, Master’s Thesis, Naval Postgraduate School, Monterey, California, 2005.

[5] A. S. Bouazzi, H. Hamzaoui, B. Rezig, “Theoretical possibilities of InGaN tandem PV structures”, *Solar Energy Materials & Solar Cells*, Vol. 87, 595-603, 2004.

[6] S. M. Sze, *Semiconductor Devices*, 2nd edition, John Wiley & Sons, Inc, 2001.

[7] Periodic table of elements, 21 March 2007, http://www.nrc-cnrc.gc.ca/student-science-tech/.

[8] Silicon atomic structure, 13 March 2007, http://www.micromountain.com/sci_diagrams/at_struct/at_struct_pages/silicon_lab_none.htm.

[9] R. F. Pierret, *Semiconductor Device Fundamentals*, Addison-Wesley Publishing, Reading, Massachusetts, 1996.

[10] J. Nelson, *The Physics of Solar Cells*, Imperial College Press, London, England, 2003.

[11] Indium Nitride and Gallium Nitride atoms per cm^3, 2 May 2007, http://www.ioffe.rssi.ru/SVA/NSM/Semicond/index.html.

[12] S. S. Hegedus and A. Luque, “Status, trends, challenges and the bright future of solar electricity from photovoltaics”, in *Handbook of Photovoltaic Science and Engineering*, Luque, A. and Hegedus S.S., eds, p. 12, John Wiley & Sons, 2003.

[13] Light spectrum, 2 May 2007, http://www1.eere.energy.gov/solar/pv_cell_light.html.

[14] Color wavelength table, 2 May 2007, http://www.usbyte.com/common/approximate_wavelength.htm.

[15] Light energy absorption with respect to band gap, 2 May 2007, http://www1.eere.energy.gov/solar/bandgap_energies.html.

[16] Simple cubic lattice structure, 24 April 2007, http://upload.wikimedia.org/wikipedia/commons/thumb/5/55/Cubic.svg/109px-Cubic.svg.png.

[17] I. Vurgaftman, J. R. Meyer, L. R. Ram–Mohan, “Band parameters for III–V compound semiconductors and their alloys”, *Applied Physics Review, Journal of Applied Physics*, Vol. 89, number 11, pp. 5815–5875, 2001.

[18] I. Vurgaftman and J. R. Meyer, “Band parameters for nitrogen-containing semiconductors”, *Journal of Applied Physics*, Volume No. 6, Number 6, pp. 3675-3696, 2003.

[19] National Renewable Energy (NREL) Air Mass Zero (AM0) solar spectrum, 17 April 2007, http://rredc.nrel.gov/solar/spectra/am0/.

[20] J. L. Gray, “The physics of the solar cell”, in *Handbook of Photovoltaic Science and Engineering*, A. Luque and S.S. Hegedus, eds, p. 12, John Wiley & Sons, 2003.

[21] F. Lasnier and T. G. Ang, *Photovoltaic Engineering Handbook*, Adam Hilger, Bristol, UK, 1990.

[22] Silvaco International, 8 May 2007, http://www.silvaco.com/products/device_simulation/atlas.html.

[23] Atlas User’s Manual, Silvaco International, 2005.

[24] V. Y. Davydov, et al., “Absorption and emission of hexagonal InN. Evidence of narrow fundamental band gap”, *Phys. Stat. Sol.* (b) 229, No. 3, R1-R3, 2002.

[25] V. Y. Davydov, et al., “Band gap of InN and In-Rich $In_xGa_{1-x}N$ alloys (0.36<x<1)”, *Phys. Stat. Sol.* (b) 230, No. 2, R4–R6, 2002.

[26] Spectrum and InGaN band gaps, 8 May 2007, http://emat-solar.lbl.gov/images/InGaN_Solar.gif.

[27] P. Specht, et al., “Band transitions in wurtzite GaN and InN determined by valence electron energy loss spectroscopy”, *Solid State Communications* 135, 340–344, 2005.

[28] W. Walukiewicz, “Native defects in InGaN alloys”, *Physica B*, 376-377, 432-435, 2006.

[29] W. Walukiewicz, “Narrow band gap group III-nitride alloys”, *Physica E* 20, 300 – 307, 2004.

[30] J. Wu, et al., “Small band gap bowing in InGaN alloys”, *Applied Physics Letters*, Volume 80, Number 25, 4741-4743, 2002.

[31] J. W. Ager III and W. Walukiewicz, “High efficiency, radiation-hard solar cells”, Lawrence Berkeley National Laboratory, Paper LBNL 56326, 2004.

[32] J. Wu and W. Walukiewicz, “Band gaps of InN and group III nitride alloys”, *Superlattices and Microstructures*, 34, 63–75, 2003.

[33] R. E. Jones, et al., “Evidence for p-type doping of InN”, Lawrence Berkeley National Laboratory, Paper LBNL 59255, 2005.

[34] P. Specht and C. Kisielowski, Dielectric constants for $In_{0.20}Ga_{0.80}N$, unpublished, 2006.

[35] R. Goldhahn, et al., “Dielectric function of “narrow” band gap InN”, *Mat. Res. Soc. Symp. Proc.* Vol. 743, L5.9.1-L5.9.6, 2003.

[36] R. R. King, et al., “Advanced III-V Multijunction Cells for space”, Spectrolab Inc, Sylmar, California, 2006.

[37] F. Bechstedt, et al., “Energy gap and optical properties of $In_xGa_{1-x}N$”, *Phys. Stat. Sol.* (a) 195, No. 3, pp. 628-633, 2003.

INITIAL DISTRIBUTION LIST

1. Defense Technical Information Center
   Ft. Belvoir, Virginia

2. Dudley Knox Library
   Naval Postgraduate School
   Monterey, California

3. Sherif Michael
   Naval Postgraduate School
   Monterey, California

4. Todd Weatherford
   Naval Postgraduate School
   Monterey, California

5. Wladek Walukiewicz
   Lawrence Berkeley National Laboratory
   Berkeley, California

6. Petra Specht
   Lawrence Berkeley National Laboratory
   Berkeley, California